

A peer-reviewed version of this preprint was published in PeerJ on 13 February 2020.

[View the peer-reviewed version](https://peerj.com/articles/8614) (peerj.com/articles/8614), which is the preferred citable publication unless you specifically need to cite this preprint.

Hervé V, Liu P, Dietrich C, Sillam-Dussès D, Stiblik P, Šobotník J, Brune A. 2020. Phylogenomic analysis of 589 metagenome-assembled genomes encompassing all major prokaryotic lineages from the gut of higher termites. PeerJ 8:e8614 <https://doi.org/10.7717/peerj.8614>

Phylogenomic analysis of 589 metagenome-assembled genomes encompassing all major prokaryotic lineages from the gut of higher termites

Vincent Hervé^{Corresp. 1}, Pengfei Liu¹, Carsten Dietrich¹, David Sillam-Dussès², Petr Stiblik³, Jan Šobotník³, Andreas Brune^{Corresp. 1}

¹ Research Group Insect Gut Microbiology and Symbiosis, Max Planck Institute for Terrestrial Microbiology, Marburg, Germany

² Laboratory of Experimental and Comparative Ethology EA 4443, Université Paris 13, Villetaneuse, France

³ Faculty of Forestry and Wood Sciences, Czech University of Life Sciences, Prague, Czech Republic

Corresponding Authors: Vincent Hervé, Andreas Brune

Email address: vincent.herve8@gmail.com, brune@mpi-marburg.mpg.de

“Higher” termites have been able to colonize all tropical and subtropical regions because of their ability to digest lignocellulose with the aid of their prokaryotic gut microbiota. Over the last decade, numerous studies based on 16S rRNA gene amplicon libraries have largely described both the taxonomy and structure of the prokaryotic communities associated with termite guts. Host diet and microenvironmental conditions have emerged as the main factors structuring the microbial assemblages in the different gut compartments. Additionally, these molecular inventories have revealed the existence of termite-specific clusters that indicate coevolutionary processes in numerous prokaryotic lineages. However, for lack of representative isolates, the functional role of most lineages remains unclear. We reconstructed 589 metagenome-assembled genomes (MAGs) from the different gut compartments of eight higher termite species that encompass 17 prokaryotic phyla. By iteratively building genome trees for each clade, we significantly improved the initial automated assignment, frequently up to the genus level. We recovered MAGs from most of the termite-specific clusters in the radiation of, e.g., Planctomycetes, Fibrobacteres, Bacteroidetes, Euryarchaeota, Bathyarchaeota, Spirochaetes, Saccharibacteria, and Firmicutes, which to date contained only few or no representative genomes. Moreover, the MAGs included abundant members of the termite gut microbiota. This dataset represents the largest genomic resource for arthropod-associated microorganisms available to date and contributes substantially to populating the tree of life. More importantly, it provides a backbone for studying the metabolic potential of the termite gut microbiota, including the key members involved in carbon and nitrogen biogeochemical cycles, and important clues that may help cultivating representatives of these understudied clades.

1 **Phylogenomic analysis of 589 metagenome-assembled**
2 **genomes encompassing all major prokaryotic lineages from**
3 **the gut of higher termites**

4

5 Vincent Hervé^{1*}, Pengfei Liu¹, Carsten Dietrich¹, David Sillam-Dussès², Petr Stiblik³, Jan
6 Šobotník³, Andreas Brune^{1*}

7

8 ¹Research Group Insect Gut Microbiology and Symbiosis, Max Planck Institute for Terrestrial
9 Microbiology, 35043 Marburg, Germany

10 ²Laboratory of Experimental and Comparative Ethology EA 4443, Université Paris 13, Sorbonne
11 Paris Cité, Villetaneuse 93430, France

12 ³Faculty of Forestry and Wood Sciences, Czech University of Life Sciences, Prague 6, Suchbát
13 16500, Czech Republic

14

15 * Corresponding authors:

16 Vincent Hervé¹

17 Research Group Insect Gut Microbiology and Symbiosis, Max Planck Institute for Terrestrial
18 Microbiology, Karl-von-Frisch-Strasse 10, 35043 Marburg, Germany

19 Email address: vincent.herve8@gmail.com

20

21 Andreas Brune¹

22 Research Group Insect Gut Microbiology and Symbiosis, Max Planck Institute for Terrestrial
23 Microbiology, Karl-von-Frisch-Strasse 10, 35043 Marburg, Germany

24 Email address: brune@mpi-marburg.mpg.de

25

26 Key words: metagenome-assembled genomes, gut microbiology, higher termites

27

28 ORCID:

29 Vincent Hervé: <http://orcid.org/0000-0002-3495-561X>

30 Andreas Brune: <http://orcid.org/0000-0002-2667-4391>

31

32 Abstract

33 “Higher” termites have been able to colonize all tropical and subtropical regions because of their
34 ability to digest lignocellulose with the aid of their prokaryotic gut microbiota. Over the last
35 decade, numerous studies based on 16S rRNA gene amplicon libraries have largely described
36 both the taxonomy and structure of the prokaryotic communities associated with termite guts.
37 Host diet and microenvironmental conditions have emerged as the main factors structuring the
38 microbial assemblages in the different gut compartments. Additionally, these molecular
39 inventories have revealed the existence of termite-specific clusters that indicate coevolutionary
40 processes in numerous prokaryotic lineages. However, for lack of representative isolates, the
41 functional role of most lineages remains unclear. We reconstructed 589 metagenome-assembled
42 genomes (MAGs) from the different gut compartments of eight higher termite species that
43 encompass 17 prokaryotic phyla. By iteratively building genome trees for each clade, we
44 significantly improved the initial automated assignment, frequently up to the genus level. We
45 recovered MAGs from most of the termite-specific clusters in the radiation of, e.g.,
46 Planctomycetes, Fibrobacteres, Bacteroidetes, Euryarchaeota, Bathyarchaeota, Spirochaetes,
47 Saccharibacteria, and Firmicutes, which to date contained only few or no representative
48 genomes. Moreover, the MAGs included abundant members of the termite gut microbiota. This
49 dataset represents the largest genomic resource for arthropod-associated microorganisms
50 available to date and contributes substantially to populating the tree of life. More importantly, it
51 provides a backbone for studying the metabolic potential of the termite gut microbiota, including
52 the key members involved in carbon and nitrogen biogeochemical cycles, and important clues
53 that may help cultivating representatives of these understudied clades.

54

55 Introduction

56 Termites (Blattodea: Termitoidae) are eusocial insects that have predominantly and successfully
57 colonized tropical and subtropical areas across the world. One of the keys to this success is their
58 rare ability to degrade lignocellulose, a very abundant but recalcitrant complex carbon substrate
59 (Cragg et al., 2015). As major decomposers, termites play an important role in carbon cycling
60 (Yamada et al., 2005; Dahlsjö et al., 2014; Liu et al., 2015; Griffiths et al., 2019). Lignocellulose
61 digestion by termites is attributed to the presence of a specific microbiota colonizing the different
62 gut compartments of the host (Brune, 2014). Even though termites produce endogenous
63 cellulases in the labial glands and/or midgut (Tokuda et al., 2004; Fujita, Miura & Matsumoto,
64 2008), the digestive processes in the hindgut are the result of microbial activities.

65 “Lower” termites feed almost exclusively on wood, whereas “higher” termites
66 (Termitidae family) diversified their diet and extended it from wood to plant litter, humus, and

67 soil (Donovan, Eggleton & Bignell, 2001). Higher termites represent the most diverse and taxon-
68 rich clade and form about 85% of the termite generic diversity (Krishna et al., 2013). Their gut
69 morphology is more complex than that of the basal clades, and is characterized by the presence
70 of a mixed-segment and an enlarged proctodeal segment P1. Moreover, the gut displays strong
71 variations in pH and oxygen partial pressure along the anterior-posterior axis, which creates
72 microenvironments within the gut (Brune, 2014).

73 Termites harbor a specific and complex gut microbiota (Brune & Dietrich, 2015;
74 Bourguignon et al., 2018). Over the last decade, numerous studies targeting the 16S rRNA gene
75 have cataloged the prokaryotic diversity of the termite gut microbiota. By analyzing the structure
76 and composition of these microbial communities, the roles of host taxonomy (Dietrich, Kohler &
77 Brune, 2014; Abdul Rahman et al., 2015), host diet (Mikaelyan et al., 2015a), and
78 microenvironments found in the different gut compartments (Mikaelyan, Meuser & Brune, 2017)
79 have emerged as the main factors shaping the termite gut microbiota. These studies have also
80 highlighted patterns of dominant taxa associated with specific diet and/or gut compartment
81 (Mikaelyan, Meuser & Brune, 2017). For instance, Spirochaetes tend to be the dominant phylum
82 in the gut of wood/grass feeders, whereas their abundance is lower in litter, humus and soil
83 feeders, in which Firmicutes are much more abundant. The accumulated 16S rRNA gene reads
84 have revealed the existence of termite-specific clusters among both bacterial and archaeal phyla
85 (e.g. among Fibrobacteres, Clostridia, Spirochaetes, and Euryarchaeota).

86 All these studies focusing on the 16S rRNA gene have helped microbiologists in
87 answering the question “who is there?”, but the following questions “what are they doing?” and
88 “who is doing what?” remain open. Attempts to answer the latter questions have been made, e.g.,
89 by analyzing different fractions of the gut content of *Nasutitermes* spp., which led to the
90 identification of fiber-associated cellulolytic bacterial taxa (Mikaelyan et al., 2014), or by
91 focusing on the diversity of individual functional marker genes, such as *nifH* (Ohkuma, Noda &
92 Kudo, 1999) or formyl-tetrahydrofolate synthetase (Ottesen & Leadbetter, 2011). The latter
93 approach, however, is problematic because the organismal origin of the respective genes is often
94 obfuscated by frequent horizontal gene transfers between prokaryotes. Thus, it has been
95 suggested that genome-centric instead of gene-centric approaches are much more relevant for
96 elucidation of soil or gut microbiotas (Prosser, 2015). Unfortunately, the number of available
97 isolates of termite gut microbiota and their genomes (Zheng & Brune, 2015; Yuki et al., 2018)
98 are low compared to those from other environments. However, modern culture-independent
99 methods, namely metagenomics and single-cell genomics have recently allowed the generation
100 of numerous metagenome-assembled genomes (MAGs) and single-amplified genomes (SAGs),
101 respectively, from uncultivated or difficult to cultivate organisms (Albertsen et al., 2013; Woyke,
102 Doud & Schulz, 2017). MAGs are becoming increasingly more prominent in the literature
103 (Bowers et al., 2017) and populate the tree of life (Parks et al., 2017). Additionally, MAGs offer
104 the opportunity to explore the metabolic potential of these organisms and to link it with their

105 ecology.

106 To date, only a limited number of MAGs and SAGs of uncultured bacteria have been
107 recovered from the guts of higher termites; these represent termite-specific lineages of
108 Fibrobacteres (Abdul Rahman et al., 2016) and Cyanobacteria (Utami et al., 2018). Here, we
109 applied a binning algorithm to 30 metagenomes from different gut compartments of eight higher
110 termite species encompassing different feeding groups to massively recover hundreds of
111 prokaryotic MAGs from these samples. After quality filtering, all these MAGs were
112 taxonomically identified within a phylogenomic framework and are discussed in the context of
113 insect gut microbiology and symbiosis.

114

115 **Materials and Methods**

116 **Metagenomic datasets**

117 To cover a wide range of microbial diversity, we used 30 metagenomic datasets representing the
118 main gut compartments (crop, midgut, P1–P5 proctodeal compartments of the hindgut) and main
119 feeding groups present in higher-termites (see Table 1). Eight species of higher termites,
120 identified by both morphological criteria and analysis of the mitogenome, were considered:
121 *Cornitermes* sp., *Cubitermes ugandensis*, *Microcerotermes parvus*, *Nasutitermes corniger*,
122 *Neocapritermes taracua*, *Termes hospes* (Dietrich & Brune, 2016), *Labiotermes labralis* and
123 *Embiratermes neotenicus* (Hervé & Brune, 2017). Field experiments were approved by the
124 French Ministry for the Ecological and Solidarity Transition (UID: ABSCH-CNA-FR-240495-
125 2). Processing of the termite samples and DNA extraction and purification were described
126 previously (Rossmassler et al., 2015). Metagenomic libraries were prepared, sequenced, quality
127 controlled, and assembled at the Joint Genome Institute (Walnut Creek, CA, USA). DNA was
128 sequenced using Illumina HiSeq 2000 or Illumina HiSeq 2500 (Illumina Inc., San Diego, CA).
129 Quality-controlled reads were assembled and uploaded to the Integrated Microbial Genomes
130 (IMG/M ER) database (Markowitz et al., 2014). Accession numbers and information about these
131 30 metagenomes can be found in Table S1.

132

133 **Genome reconstruction**

134 For each metagenomic dataset, both quality-controlled (QC) and assembled (contigs) reads were
135 downloaded from IMG/M ER in August 2017. To obtain coverage profile of contigs from each
136 metagenomic assembly, the QC reads were mapped to contigs using BWA v0.7.15 with the bwa-
137 mem algorithm (Li & Durbin, 2009). This generated SAM files that were subsequently converted
138 into BAM files using SAMtools v1.3 (Li et al., 2009). Combining coverage profile and
139 tetranucleotide frequency information, genomes were reconstructed from each metagenome with

140 MetaBAT version 2.10.2 with default parameters (Kang et al., 2019). Quality of the
141 reconstructed genomes was estimated with CheckM v1.0.8 (Parks et al., 2015). Only MAGs that
142 were at least 50% complete and with less than 10% contamination, were retained for subsequent
143 analyses. These MAGs have been deposited at GenBank under the BioProject accession number
144 PRJNA560329; genomes are available with accession numbers SRR9983610-SRR9984198
145 (Table S2). For each MAG, CheckM was also used to extract 16S rRNA gene sequences as well
146 as a set of 43 phylogenetically informative marker genes consisting primarily of ribosomal
147 proteins and RNA polymerase domains. Finally, CheckM was also used for a preliminary
148 taxonomic classification of the MAGs by phylogenetic placement of the MAGs into the CheckM
149 reference genome tree. When available, 16S rRNA gene sequences were classified using the k-
150 nearest neighbor (knn) algorithm implemented in mothur v1.39.5 (Schloss et al., 2009) and the
151 BLASTN search method with the SILVA reference database release 132 (Quast et al., 2013) and
152 DictDb v3 (Mikaelyan et al., 2015b).

153

154 **Phylogenomic analysis**

155 In order to improve the initial CheckM classification, genome trees were built for each clade of
156 interest (from kingdom to family level). Using this initial CheckM classification and when
157 available, the 16S rRNA gene classification, genomes of closely related organisms and relevant
158 outgroups were manually selected and downloaded from NCBI and IMG/M ER. These genomes
159 were subjected to a similar CheckM analysis to extract a set of 43 single-copy marker genes, to
160 translate them into amino acid sequences, and to create a concatenated fasta file (6,988
161 positions). For each clade of interest, the amino acid sequences from the MAGs, their relatives,
162 and outgroups were aligned with MAFFT v7.305b and the FFT-NS-2 method (Kato &
163 Standley, 2013), and the resulting alignment was filtered using trimAL v1.2rev59 with the
164 gappyout method (Capella-Gutierrez et al., 2009). Smart Model Selection (Lefort, Longueville &
165 Gascuel, 2017) was used to determine the best model of amino acid evolution of the filtered
166 alignment based on Akaike Information Criterion. Subsequently, a maximum-likelihood
167 phylogenetic tree was built with PhyML 3.0 (Guindon et al., 2010). Branch supports were
168 calculated using a Chi²-based parametric approximate likelihood-ratio test (aLRT) (Anisimova
169 & Gascuel, 2006). Finally, each tree was visualized and edited with iTOL (Letunic & Bork,
170 2019). Following the procedure described above, a genome tree containing only the MAGs
171 generated in the present study was also built and visualized with GraPhlAn version 0.9.7
172 (Asnicar et al., 2015).

173

174 Estimation of the relative abundance of the MAGs in each metagenome

175 For each metagenome, raw reads were mapped against assembled contigs using BWA (Li &
176 Durbin, 2009) with default parameters. Unmapped reads and reads mapped to more than one
177 location were removed by using SAMtools (Li et al., 2009) with parameters: F 0x904. Reads
178 mapped to each contigs were summarized using the “pileup.sh” script (BBmap 38.26) (Bushnell,
179 2014). To determine the relative abundance of each MAG in the metagenome from which it was
180 binned, reads mapped to all contigs belonging to each MAG were calculated. The relative
181 abundance of one MAG was estimated by dividing all reads mapped to the MAG by all reads
182 mapped to all contigs in the metagenomes. Similarly, the MAG coverage was estimated by
183 multiplying the mapped reads by the read length and dividing it by the MAG length.

184

185 Statistical analyses

186 Statistical analyses were performed with R version 3.4.4 (R Development Core Team, 2015), and
187 data were visualized with the *ggplot2* (Wickham, 2016) package. Correlations between
188 quantitative variables were investigated with Pearson's product moment correlation coefficient.

189

190 Results and Discussion

191 Metagenomes and MAGs overview

192 Metagenomic reads were generated from the P1, P3 and P4 proctodeal compartments of the gut
193 of the two termite species *Embiratermes neotenicus* and *Labiotermes labralis*. These six
194 metagenomes were combined with 24 previously published metagenomes from the gut of higher
195 termites (Rossmassler et al., 2015) in order to obtain data encompassing different gut
196 compartments from eight species of higher termites feeding on different lignocellulosic
197 substrates ranging from wood to soil (Table 1). Metagenomic binning of these 30 termite gut
198 metagenomes yielded 1732 bins in total (Table S1). For further analysis, we selected only those
199 bins that represented high-quality (135 bins, >90% complete and <5% contamination) and
200 medium-quality (454 bins, >50% complete and <10% contamination) MAGs (Table 1, Table
201 S1). The present study focused on these 589 MAGs, which showed on average a 38.6-fold
202 coverage (Table S2).

203 The number of MAGs recovered from the different metagenomes did not show a
204 Gaussian distribution. Instead, we found a significant and positive relationship between the
205 number of metagenome-assembled reads and the number of MAGs recovered ($r = 0.85$,
206 $p < 0.0001$), indicating that assembly success and sequencing depth were important predictors of
207 genome reconstruction success (Figure 1). This is in agreement with benchmarking reports on
208 metagenomic datasets (Sczyrba et al., 2017) and underscore that a good quality assembly is a

209 prerequisite for high binning recovery, which is important to consider when designing a
210 metagenomic project for the purpose of binning. A significantly higher number of assembled
211 reads and of MAGs recovered was observed in the current dataset compared to the Rossmasser
212 et al., 2015 dataset (Wilcoxon test, $p < 0.005$), highlighting the importance of this new dataset
213 (Figure 1).

214 **MAGs taxonomy and abundance**

215 We investigated the phylogenomic context of the 589 MAGs. An initial automated classification
216 of the MAGs using CheckM and when available, the taxonomic assignment of the 16S rRNA
217 gene, identified representatives of 15 prokaryotic phyla (Table S3). Initially, 142 MAGs (24% of
218 the dataset) remained unclassified at the phylum level, and key taxa of the termite microbiota,
219 such as Fibrobacteres and *Treponema*, were absent or only poorly represented. This is partly
220 explained by the lack of representative genomes for certain taxa in the reference genome tree
221 provided in the current version of CheckM (e.g., only one Fibrobacteres genome and one
222 Elusimicrobia genome, and an absence of Bathyarchaeota and Kiritimatiellaeota genomes). New
223 tools incorporating larger databases, such as GTDB-Tk (Parks et al., 2018), will probably resolve
224 such issues.

225 We improved the taxonomic resolution of the classification by iteratively constructing
226 genome trees for each clade of interest that included all recently published reference genomes.
227 This approach allowed the successful classification of all 589 MAGs at least at the phylum level
228 and in some cases down to the genus level (Table S2). Thirty-eight MAGs were from the
229 archaeal domain, and 551 MAGs were from the bacterial domain, which together represented a
230 total of 17 prokaryotic phyla (Figure 2). Obvious patterns in the taxonomic distribution of the
231 MAGs according to the sample origin were not apparent, which reflects the lack of effects of the
232 gut compartments and/or of the diet of the host on the genome taxonomy (Figures S1 and S2).
233 Among the most abundant phyla, genomes were recovered from different gut compartments and
234 diets, which indicated a good coverage of the diversity among gut compartments and host diets.

235 We computed the relative abundance of each MAG. These abundances ranged from 0.005%
236 to 4.63% (Table S2), with a mean value of 0.23%, which can be considered as abundant
237 (Delmont et al., 2018). The average mean value indicated that the present dataset includes
238 abundant members of the termite gut microbiota, which was confirmed when we looked at the
239 taxonomic distribution of the MAGs (Figure 3), in particular when we linked it to the host diet.
240 Indeed, similarities were observed when we compared taxonomic patterns of the MAG relative
241 abundance with previously published 16S rRNA gene amplicon-based surveys (Abdul Rahman
242 et al., 2015; Mikaelyan, Meuser & Brune, 2017). For instance, Spirochaetes were the most
243 abundant phylum within the wood-feeding termite *Nasutitermes corniger*, and their proportion
244 decreases along the humification gradient, being less abundant in the gut of humus feeders and
245 litter feeders and even less abundant in soil feeders, in the favor of other phyla such as

246 Firmicutes. Fibrobacteres were preferentially abundant within wood- and litter-feeder samples.
247 Interestingly, a significant and negative relationship between the number of metagenome-
248 assembled reads and the MAG relative abundance ($r = -0.34$, $p < 0.0001$) was observed. This
249 could be partly explained by the fact that increasing sequencing depth would increase the number
250 of metagenome-assembled reads and thus allow the binning of sequences from less abundant
251 organisms. However, since quantity of metagenome-assembled reads and relative abundance are
252 not independent variables, it also implies that MAG relative abundances can not be directly
253 quantitatively compared between samples but only within a single sample. Thus, proportions of
254 taxa within a sample using relative abundance can be used to describe such sample.

255 Archaea

256 The archaeal domain was represented by members of the phyla Euryarchaeota and
257 Bathyarchaeota (Figure 4, Figure S3). Euryarchaeota were represented by 23 MAGs that were
258 classified as members of the genera *Methanobrevibacter* (family *Methanobacteriaceae*; 3
259 MAGs) and, *Methanimicrococcus* (family *Methanosarcinaceae*; 3 MAGs), and members of the
260 family *Methanomassiliicoccaceae* (16 MAGs), one of them in the genus *Candidatus*
261 *Methanoplasma*. MAGs assigned as Euryarchaeota encompassed three (*Methanobacteriales*,
262 *Methanosarcinales*, and *Methanomassiliicoccales*) of the four orders of methanogens found in
263 termite guts (Brune, 2018); *Methanomicrobiales* were absent from the present dataset. This
264 genomic resource will be extremely valuable for a better understanding of the genomic basis of
265 methanogenesis in the termite gut and more generally for investigating the functional role of
266 archaea in arthropod guts. Indeed, Euryarchaeota have been found to be present in virtually all
267 termite species investigated (Brune, 2018), and a global 16S rRNA gene survey has revealed that
268 this phylum is the most abundant archaeal clade in arthropod-associated microbiota (Schloss et
269 al., 2016). Bathyarchaeota were represented by 15 MAGs, which formed a termite-specific
270 cluster, with Bathyarchaeota reconstructed from sediments of the White Oak River (WOR)
271 estuary (North Carolina, USA) as next relatives (Lazar et al., 2016) (Figure 4). Bathyarchaeota is
272 a lineage formerly known as Miscellaneous Crenarchaeota Group (MCG), which has been
273 reported to occur in the gut of soil-feeding termites (Friedrich et al., 2001). To date, MAGs of
274 Bathyarchaeota have been mostly derived from aquatic environments (Zhou et al., 2018). Here,
275 we identify the members of this lineage as Bathyarchaeota and provide the first genomes from
276 this environment. Interestingly, Bathyarchaeota MAGs were particularly abundant in humus-,
277 litter- and soil-feeding termites (Figure 3); a genomic characterization, combined with analyses
278 of their abundance and localization, should shed light on the metabolic potential of these
279 organisms and their functional role in termite guts.

280 Firmicutes

281 Firmicutes was by far the most abundantly represented phylum. The 237 MAGs (40% of the total
282 dataset) represented three classes (*Bacilli*, *Clostridia* and *Erysipelotrichia*) and ten families,

283 including four members of *Streptococcaceae* (*Bacilli*) and three members of *Turicibacteraceae*
284 (*Erysipelotrichia*). *Clostridia* was the most diverse and rich class (191 MAGs), in which
285 *Ruminococcaceae* (91 MAGs), *Defluviitaleaceae* (64 MAGs), *Lachnospiraceae* (4 MAGs),
286 *Peptococcaceae* (4 MAGs), *Eubacteriaceae* (2 MAGs), *Symbiobacteriaceae* (2 MAGs), Family
287 XIII *incertae sedis* (2 MAGs) and *Clostridiales incertae sedis* (2 MAGs) families were
288 identified. Interestingly, among the *Defluviitaleaceae*, the genomes were mainly recovered from
289 the P1 compartment (51 MAGs, i.e., 80% of the family members) whereas *Ruminococcaceae*
290 were predominantly recovered from the P3 compartment (58 MAGs, i.e., 64% of the family
291 members). Further studies should investigate the potential metabolic specialization of these two
292 families in relation to the gut physicochemical properties. A fourth class-level lineage could not
293 be further classified for lack of reference genomes. In a recent global 16S rRNA gene-based
294 survey, it has been suggested that many novel lineages of Firmicutes in insect-associated
295 metagenomes are hidden (Schulz et al., 2017). Our present study confirms this idea but our
296 genome trees also provide evidence of new lineages. Here we report the first genomes of
297 uncultured termite-specific lineages that were already detected in previous 16S rRNA gene-
298 based surveys (Bourguignon et al., 2018). For example, the phylogenomic tree of the most
299 abundant family *Ruminococcaceae* (Figure S4) showed various termite-specific clusters,
300 including a cluster of 18 MAGs closely related to *Sporobacter termitidis* isolated from
301 *Nasutitermes lujae* (Grech-Mora et al., 1996). *Lachnospiraceae*, *Ruminococcaceae*,
302 *Turicibacteraceae* (previously classified as *Erysipelotrichaceae*), and *Defluviitaleaceae*
303 (previously classified as *Lachnospiraceae*) have been reported among the dominant taxa in
304 termite guts (Mikaelyan, Meuser & Brune, 2017), but most of them remain uncultivated and/or
305 with few representative genomes. As such, many questions regarding their ecology and
306 metabolism remain open. With 237 Firmicutes MAGs recovered from different gut
307 compartments and from hosts with different diets, the present study provides the material for
308 further genomic exploration of the role of these bacteria in plant polysaccharide degradation,
309 based for instance on CAZyme distribution (Lombard et al., 2014). Since diet has been shown to
310 be the main factor shaping gut community composition in higher termites (Mikaelyan et al.,
311 2015a), one might hypothesize the existence of different arsenals of lignocellulolytic enzymes,
312 potentially reflecting the host diet specificity (balance between cellulose, lignin, and
313 hemicelluloses). More generally, Firmicutes and especially *Ruminococcaceae* are also abundant
314 and metabolically important in rumen systems (Svartström et al., 2017; Söllinger et al., 2018;
315 Stewart et al., 2018). At a broader scale, our dataset will allow comparative studies between
316 intestinal tract microbiota of ruminants and phytophagous or xylophagous invertebrates, which
317 would allow a better understanding of plant polysaccharide degradation across the tree of life.

318 **Actinobacteria**

319 Actinobacteria was the second most abundant phylum with 71 MAGs, including members of the
320 classes *Acidimicrobiia*, *Actinobacteria*, *Coriobacteriia* and *Thermoleophilia* (Figure S5). Eight

321 families were represented, namely *Propionibacteriaceae* (11 MAGs), *Promicromonosporaceae*
322 (4 MAGs), *Eggerthellaceae* (4 MAGs), *Microbacteriaceae* (2 MAGs), *Nocardoidaceae* (2
323 MAGs), *Acidimicrobiaceae* (1 MAG), *Nocardiaceae* (1 MAG) and *Conexibacteraceae* (1
324 MAG). Among these 71 MAGs, 36 were recovered from humus feeders, 33 from soil feeders but
325 only 2 from wood feeders, which suggests a higher prevalence in termites with a more humified
326 diet. This phylum is known to be present and of significant abundance in both the nest (Sujada,
327 Sungthong & Lumyong, 2014) and gut of termites (Le Roes-Hill, Rohland & Burton, 2011), but
328 to be more abundant in the nest (Moreira et al., 2018). This was for instance the case for the
329 families *Acidimicrobiaceae*, *Nocardiaceae*, *Promicromonosporaceae*, *Microbacteriaceae*,
330 *Nocardoidaceae*, and *Propionibacteriaceae*, which were more abundant in the nest than in the
331 gut of workers or soldiers of *Procornitermes araujo* (Moreira et al., 2018). Therefore, one of the
332 key questions regarding this phylum concerns their effective role in lignocellulose degradation in
333 the termite guts. Are they just present in the surrounding environment of the termite and thus
334 sometimes transit from the gut or are they actively involved in food digestion? The MAGs
335 obtained in the present study will allow to address such questions by evaluating gene expression
336 of these organisms using metatranscriptomic data from higher termites (He et al., 2013;
337 Marynowska et al., 2017).

338 **Spirochaetes**

339 The phylum Spirochaetes was represented by 68 MAGs from wood-, soil-, litter- and humus-
340 feeding termites. It has long been known that Spirochaetes are a diverse and important lineage in
341 termite gut (Paster et al., 1996; Lilburn, Schmidt & Breznak, 1999), especially because of their
342 involvement in reductive acetogenesis (Leadbetter et al., 1999; Ohkuma et al., 2015) and in
343 hemicellulose degradation (Tokuda et al., 2018). In terms of abundance, Spirochaetes are among
344 the dominant phyla in termite guts and may represent more than half of the bacterial relative
345 abundance in some species (Diouf et al., 2018a). Three Spirochaetes orders, namely
346 *Brevinematales* (1 MAG), *Leptospirales* (4 MAGs) and *Spirochaetales* (59 MAGs), were
347 identified (Figure 5, Figure S6). In the latter order, 54 MAGs recovered from the P1, P3 and P4
348 compartments of wood-, litter-, humus-, and soil-feeding hosts were assigned to the termite-
349 specific cluster *Treponema* I (Ohkuma, Iida & Kudo, 1999; Lilburn, Schmidt & Breznak, 1999)
350 and represent the first genomes of this cluster from higher termites. Indeed, to date only two
351 *Treponema* I genomes are available, and both were recovered from isolates, namely
352 *T. azotonutricium* and *T. primitia*, from the hindgut of the lower termite *Zootermopsis*
353 *angusticollis* (Graber, Leadbetter & Breznak, 2004). Thus, our dataset significantly expands the
354 genomic resources for this taxonomic group. Subclusters of this clade have been identified on a
355 dedicated genome tree (Figure 5). The genome tree topology is in agreement with a previous
356 phylogenomic Spirochaetes study (Gupta, Mahmood & Adeolu, 2013). Regarding Spirochaetes
357 classification, our tree topology suggests that the genus *Treponema* could be elevated at least to
358 the family rank due to the presence of distinct *Treponema* clusters (Figure 5). This observation is

359 also in agreement with the recent Genome Taxonomy Database, which now proposes a
360 *Treponemataceae* family and a *Treponematales* order (Parks et al., 2018).

361 **Fibrobacteres**

362 Thirteen members of the Fibrobacteres phylum were recovered from the P1, P3, and P4
363 compartments of wood-, litter-, humus-, and soil-feeding termites. These genomes encompass
364 the 3 classes of this phylum, namely *Chitinispirillia* (5 MAGs), *Chitinivibrionia* (previously
365 known as TG3 candidate phylum; 2 MAGs), and *Fibrobacteria* (6 MAGs) (Figure 6, Figure S7).
366 Phylogenomic analysis of this phylum suggests the existence of a termite-specific cluster among
367 *Fibromonadales* (Figure 6). This is in agreement with a previous 16S rRNA gene-based
368 phylogenetic analysis and a phylogenomic analysis that identify the family *Fibromonadaceae* as
369 a termite-specific cluster within this order (Abdul Rahman et al., 2016). Members of the phylum
370 Fibrobacteres are abundant in the hindgut of wood-feeding higher termites (Hongoh et al., 2006),
371 where they have been identified as fiber-associated cellulolytic bacteria (Mikaelyan et al., 2014).
372 To date, available Fibrobacteres genomes from termite guts belong to *Chitinivibrionia*
373 (previously classified as TG3 phylum) and *Fibrobacteria* (Abdul Rahman et al., 2016). Here we
374 also added five members of *Chitinispirillia* to the list of termite-associated Fibrobacteres
375 genomes. Interestingly, we did not recover MAGs within the *Fibrobacterales*, which harbors the
376 *Fibrobacter* genus, a clade that was also absent from 16S rRNA gene-based surveys of termite
377 gut microbiota (Hongoh et al., 2006; Mikaelyan et al., 2015b; Bourguignon et al., 2018).
378 Members of this genus have been isolated from the gastrointestinal tracts of mammals and bird
379 herbivores (Neumann, McCormick & Suen, 2017), where they are potentially involved in
380 cellulose and hemicellulose degradation (Neumann & Suen, 2018). This suggests co-evolution
381 patterns among different Fibrobacteres clades within animal hosts with a lignocellulose-based
382 diet.

383 **Proteobacteria and Bacteroidetes**

384 Sixty-seven MAGs of Proteobacteria belonging to *Alphaproteobacteria* (21 MAGs),
385 *Betaproteobacteria* (15 MAGs), and *Deltaproteobacteria* (21 MAGs) were recovered from all
386 hindgut compartments of litter-, humus-, and soil-feeding termites. Among the
387 *Deltaproteobacteria*, six orders were identified, namely *Desulfobacterales* (3 MAGs, all
388 assigned to *Desulfobulbus*), *Desulfovibrionales* (5 MAGs), *Desulfuromonadales* (1 MAG),
389 *Myxococcales* (4 *Cystobacterineae* and 4 *Polyangiaceae*), Rs-K70 group (1 MAG), and
390 *Syntrophobacterales* (1 *Syntrophaceae* and 2 *Syntrophorhabdaceae*). *Desulfovibrionaceae*
391 (*Desulfovibrionales*) members of gut and termite-gut clusters have been found to be highly
392 prevalent in termite guts (Bourguignon et al., 2018). Similarly, we identified 3
393 *Desulfovibrionaceae* MAGs that form a monophyletic clade and 2 *Desulfovibrionaceae* MAGs
394 that fall into a cluster of gut-associated genomes (Figure S8). This family, among others, is
395 composed of various sulfate-reducing bacteria; this functional group has already been identified

396 in different termite species (Kuhnigk et al., 1996). Thus, these MAGs could provide new
397 genomic resources to further investigate this metabolism in the termite gut.

398 Our dataset comprises 33 MAGs of Bacteroidetes (Figure S9), including members of the
399 families *Candidatus* Azobacteroides (4 MAGs), *Lentimicrobiaceae* (5 MAGs),
400 *Paludibacteraceae* (2 MAGs, both assigned to the *Paludibacter* genus), *Rikenellaceae* (2
401 MAGs), *Marinilabiliaceae* (1 MAG), and *Prolixibacteraceae* (1 MAG). These Bacteroidetes
402 were found in the P1, P3, and P4 compartments and in wood-, litter-, humus-, and soil-feeding
403 termites. In Blattodea guts, different clusters of *Alistipes* (Bacteroidetes) have been found in a
404 16S rRNA gene survey (Mikaelyan et al., 2015b). Two MAGs from *Labiotermes labralis*
405 belonging to the *Rikenellaceae* family and closely related to *Alistipes* have been identified.
406 Additionally, among Bacteroidetes, four MAGs, all originating from P4 compartments, fall into
407 the *Candidatus* Azobacteroides family that contains symbionts of flagellates from guts of lower
408 termites (Hongoh et al., 2008b; Yuki et al., 2015). We also recovered two MAGs assigned to
409 *Paludibacter*; *Paludibacter propionicigenes* and *Paludibacter jiangxiensis* are both strictly
410 anaerobic, propionate-producing bacteria isolated from rice paddy field (Ueki et al., 2006; Qiu et
411 al., 2014). Propionate is produced by fermenting bacteria in the gut of termites (Odelson &
412 Breznak, 1983); these bacteria utilize glucose generated by cellulose degradation to form
413 succinate and propionate (Tokuda et al., 2014). *P. propionicigenes* might be involved in nitrogen
414 fixation, as *nifH* transcripts assigned to this species are the most abundant in the gut of the wood-
415 feeding beetle *Odontotaenius disjunctus* (Ceja-Navarro et al., 2014).

416 **Saccharibacteria, Synergistetes and Planctomycetes**

417 Fifteen MAGs of *Candidatus* Saccharibacteria (also known as candidate division TM7) were
418 reconstructed from the P1, P3, and P4 compartments of wood-, litter-, humus- and soil-feeding
419 termites (Figure S10). Most of them originated from humus feeders (11 MAGs), especially from
420 the P3 compartment (8 out of these 11 MAGs). Similarly, six MAGs of Synergistetes, all
421 belonging to the *Synergistaceae* family that contains a termite/cockroach cluster (Mikaelyan et
422 al., 2015b), were recovered from the P3 and P4 compartments of humus- and soil-feeding
423 termites (Figure S11). Both Saccharibacteria and Synergistetes were recently highlighted as
424 numerically important clades of the termite gut microbiota, with some OTUs being present in the
425 gut of the majority of 94 termite species collected across four continents (Bourguignon et al.,
426 2018). Genomic analysis of these MAGs should help in understanding the roles of these bacteria
427 in termite gut and also provide clues for designing successful isolation media to study their
428 physiology.

429 Twelve MAGs were assigned to the phylum Planctomycetes, including 4 to the class
430 *Phycisphaerae* (and among them 2 classified as *Phycisphaerales*) and 7 to the class
431 *Planctomycetia* (all classified as *Planctomycetaceae*) (Figure S12). These MAGs were recovered
432 from the P3, P4, and P5 compartments and were restricted to humus- and soil-feeding termites.

433 The recovery of Planctomycetes was expected, especially from the *Planctomycetaceae* family,
434 which also contains a termite / cockroach cluster (Mikaelyan et al., 2015b). Interestingly, we
435 found three MAGs from the P4 and P5 compartments of *Cubitermes ugandensis*, with one 16S
436 rRNA gene sequence assigned to the termite/cockroach cluster 2 (according to DictDb v3.0
437 classification), described in a previous study investigating the gut microbiota of the same termite
438 species (Köhler et al., 2008). When such 16S rRNA gene information is available, it will allow
439 the direct linkage between prokaryotic taxonomy and potential metabolisms.

440 **Other phyla**

441 Nine members of the phylum Elusimicrobia were identified, including members of the class
442 *Endomicrobia* (7 members) and *Elusimicrobia* (1 member) (Figure S13). These were found in all
443 hindgut compartments and were restricted to humus- and soil-feeding termites. Currently, only
444 three complete genomes of Elusimicrobia from insect guts are available: *Elusimicrobium*
445 *minutum* from the gut of a humivorous scarab beetle larva (Herlemann et al., 2009), and
446 *Endomicrobium proavitum* (Zheng & Brune, 2015) and *Candidatus Endomicrobium*
447 *trichonymphae* (Hongoh et al., 2008a) from the termite gut. Here, we provided 9 additional
448 genomes from the guts of humus- and soil-feeding termites.

449 The Chloroflexi phylum was represented by eight MAGs, including seven belonging to
450 the class *Dehalococcoidia*, found exclusively in the P3 and P4 compartments of humus- and soil-
451 feeding termites (Figure S10). Their function in termite gut remains unclear, but Chloroflexi,
452 including *Dehalococcoidia*, were found to be enriched in lignin-amended tropical forest soil
453 (DeAngelis et al., 2011), where oxygen concentration and redox potential are highly variable, as
454 in the termite gut (Brune, 2014). Therefore, their ability to use oxygen as final electron acceptor
455 and their potential involvement in lignin degradation could be investigated by comparative
456 genomics.

457 Minor phyla were also present in our dataset. Two MAGs assigned as Cloacimonetes
458 (Figure S14) and five MAGs assigned as Kiritimatiellaeota were recovered from the P3
459 compartment of the two humus-feeding termites *Neocapritermes taracua* and *Termes hospes*
460 (Figure S15). Kiritimatiellaeota have been reported to be present in the digestive tract of various
461 animals (Spring et al., 2016). The few clones obtained from termite guts, which had been
462 tentatively classified as uncultured Verrucomicrobia, were mostly obtained with planctomycete-
463 specific primers (Köhler et al., 2008), underscoring the potential biases in amplicon-based
464 studies toward certain taxa. Similarly, one MAG of Microgenomates (also known as candidate
465 division OP11), which probably represents a lineage of Pacebacteria that was discovered only in
466 a recent amplicon-based analysis but occurs in the majority of termites investigated
467 (Bourguignon et al., 2018), was reconstructed from the P3 compartment of *Termes hospes*
468 (Figure S10).

469 Finally, four MAGs classified as Acidobacteria were reconstructed from either the P3 or

470 P4 compartments of humus- and soil-feeding termites (Figure S16), which show a moderately
471 alkaline or circumneutral pH in comparison to the highly alkaline P1. Of these four genomes,
472 two were assigned to the family *Holophagaceae* and one to the *Acidobacteriaceae*.
473 Acidobacteria can represent a significant fraction of the termite gut microbiota, especially in
474 wood-feeding termites (Hongoh et al., 2005; Wang et al., 2016; Bourguignon et al., 2018).
475 Moreover, *Holophagaceae* and *Acidobacteriaceae* have been reported to be present in
476 moderately acidic lignocellulosic substrates, such as peatland soil (Schmidt et al., 2015) and
477 decaying wood (Hervé et al., 2014). Genomic analysis should help us in identifying the
478 metabolic potential of these MAGs for lignocellulose degradation.

479 **Phyla not represented by MAGs**

480 Several bacterial phyla and one archaeal phylum containing prominent taxa that have been
481 identified in previous 16S rRNA gene surveys of termite guts were not represented among the
482 MAGs recovered in the present study. They include Cyanobacteria (class *Melainabacteria*;
483 Utami et al., 2018), Lentisphaerae (Köhler et al., 2012; Sabree & Moran, 2014),
484 Verrucomicrobia (Wertz et al., 2012), and Thaumarchaeota (Friedrich et al., 2001; Shi et al.,
485 2015). Also intracellular symbionts of termite tissues, such as *Wolbachia* (Proteobacteria) (Diouf
486 et al., 2018b) were not recovered. Possible reasons are a low relative abundance and/or a high
487 phylogenetic diversity of the respective lineages. Although larger metagenomes should improve
488 the chances of their recovery in the medium- and high-quality bins, targeted single-cell based
489 approaches have proven to be quite effective in recovering these genomes (Ohkuma et al., 2015;
490 Yuki et al., 2015; Utami et al., 2019).

491

492 **Conclusions**

493 The 589 MAGs reported here represent the largest genomic resource for arthropod-associated
494 microorganisms available to date. Moreover, almost all major prokaryotic lineages previously
495 identified in 16S rRNA gene amplicon-based surveys of the gut of higher termites were
496 recovered from our 30 metagenomes. This provides the foundations for studying the prokaryotic
497 metabolism of the termite gut microbiota, including the key members involved in carbon and
498 nitrogen biogeochemical cycles, and important clues that may help in cultivating representatives
499 of these understudied clades.

500

501 **Acknowledgments**

502 The authors thank all JGI staff, particularly their project manager Tijana Glavina del Rio, for
503 their excellent service. The technical assistance of Katja Meuser is highly appreciated.

504

505

506 **Tables**

507 **Table 1. Recovery of metagenome-assembled genomes (MAGs) from the 30 termite gut**
508 **metagenomes analyzed in this study.** The host termite, its mitochondrial genome accession
509 number, dietary preference, and the originating gut compartments are indicated. *C* crop (foregut),
510 *M* midgut, *P1–P5* proctodeal compartments (hindgut). The sample codes used for the
511 metagenomes are the combination of host ID and gut compartment.

512

513 **Figure legends**

514 **Figure 1: Relationship between the number of MAGs recovered and the number of**
515 **assembled reads in the respective metagenomes.** The linear regression line and the Pearson
516 correlation coefficient (r) are shown for the entire dataset.

517 **Figure 2: Distribution of the 589 MAGs among bacterial and archaeal phyla.** This
518 maximum-likelihood tree was inferred from a concatenated alignment (amino acids) of 43
519 protein-coding genes using the LG+G+I model of evolution.

520 **Figure 3: Relative abundance of the MAGs from different phyla among the respective**
521 **metagenomes.** Circle size indicates the relative abundance of the MAGs among the respective
522 metagenome sample; color indicates host diet.

523 **Figure 4: Phylogenomic tree of the archaeal domain.** This maximum-likelihood tree was
524 inferred from a concatenated alignment of 43 proteins using the LG+G+I+F model of amino-acid
525 evolution. Branch supports were calculated using a Chi2-based parametric approximate
526 likelihood-ratio test. Names in bold included MAGs recovered in the present study. Clusters
527 shaded in brown consist exclusively of MAGs from termite guts and clusters shaded in gray
528 contain genomes from termite guts. The Asgard group was used as outgroup.

529 **Figure 5: Phylogenomic tree of the Spirochaetes phylum.** This maximum-likelihood tree was
530 inferred from a concatenated alignment of 43 proteins using the LG+G+I+F model of amino-acid
531 evolution. Branch supports were calculated using a Chi2-based parametric approximate
532 likelihood-ratio test. Names in bold included MAGs recovered in the present study. Clusters
533 shaded in brown consist exclusively of genomes from termite guts and clusters shaded in gray
534 contain genomes from termite guts. Elusimicrobia and Cyanobacteria were used as outgroup.

535 **Figure 6: Phylogenomic tree of the Fibrobacteres phylum.** This maximum-likelihood tree was
536 inferred from a concatenated alignment of 43 proteins using the LG+G+I+F model of amino-acid
537 evolution. Branch supports were calculated using a Chi2-based parametric approximate
538 likelihood-ratio test. Names in bold included MAGs recovered in the present study. Clusters

539 shaded in brown consist exclusively of genomes from termite guts and clusters shaded in gray
540 contain genomes from termite guts. Bacteroidetes were used as outgroup.

541

542

543 **Supplementary information**

544 **Supplementary Table S1:** Metagenome characteristics.

545 **Supplementary Table S2:** Final taxonomic assignment and characteristics of the MAGs

546 **Supplementary Table S3:** Initial taxonomic assignment of the MAGs

547 **Figure S1: Phylogenomic distribution of the MAGs according to the host diet.** The outer
548 rings show the occurrence of MAGs in termites with different diets. The maximum likelihood
549 tree was inferred from a concatenated alignment of 43 proteins using the LG+G+I model of
550 amino-acid evolution.

551 **Figure S2: Phylogenomic distribution of the MAGs according to the gut compartment of
552 the host.** The outer rings show the occurrence of MAGs in the different termite gut
553 compartments: *C* crop (foregut), *M* midgut, *PI–P5* proctodeal compartments (hindgut). The
554 maximum-likelihood tree was inferred from a concatenated alignment of 43 proteins using the
555 LG+G+I model of amino-acid evolution.

556 **Figure S3: Phylogenomic tree of the Archaea.** This maximum-likelihood tree was inferred
557 from a concatenated alignment of 43 proteins using the LG+G+I+F model of amino-acid
558 evolution. Branch supports were calculated using a Chi2-based parametric approximate
559 likelihood-ratio test. Asgard group was used as outgroup. Names in bold included MAGs
560 recovered in the present study.

561 **Figure S4: Phylogenomic tree of the *Ruminococcaceae* family (Firmicutes).** This maximum-
562 likelihood tree was inferred from a concatenated alignment of 43 proteins using the LG+G+I
563 model of amino-acid evolution. Branch supports were calculated using a Chi2-based parametric
564 approximate likelihood-ratio test. *Dorea* and *Butyrivibrio* (*Lachnospiraceae*) species were used
565 as outgroup. Names in bold included MAGs recovered in the present study.

566 **Figure S5: Phylogenomic tree of the Actinobacteria.** This maximum-likelihood tree was
567 inferred from a concatenated alignment of 43 proteins using the LG+G+I+F model of amino-acid
568 evolution. Branch supports were calculated using a Chi2-based parametric approximate
569 likelihood-ratio test. Chloroflexi species were used as outgroup. Names in bold included MAGs
570 recovered in the present study.

571 **Figure S6: Phylogenomic tree of the Spirochaetes.** This maximum-likelihood tree was inferred
572 from a concatenated alignment of 43 proteins using the LG+G+I+F model of amino-acid

573 evolution. Branch supports were calculated using a Chi2-based parametric approximate
574 likelihood-ratio test. Elusimicrobia and Cyanobacteria were used as outgroup. Names in bold
575 included MAGs recovered in the present study.

576 **Figure S7: Phylogenomic tree of the Fibrobacteres.** This maximum-likelihood tree was
577 inferred from a concatenated alignment of 43 proteins using the LG+G+I+F model of amino-acid
578 evolution. Branch supports were calculated using a Chi2-based parametric approximate
579 likelihood-ratio test. Bacteroidetes were used as outgroup. Names in bold included MAGs
580 recovered in the present study.

581 **Figure S8: Phylogenomic tree of the *Desulfovibrionaceae* family (*Deltaproteobacteria*).** This
582 maximum-likelihood tree was inferred from a concatenated alignment of 43 proteins using the
583 LG+G+I model of amino-acid evolution. Branch supports were calculated using a Chi2-based
584 parametric approximate likelihood-ratio test. *Desulfonatronum* species were used as outgroup.
585 Names in bold included MAGs recovered in the present study.

586 **Figure S9: Phylogenomic tree of the Bacteroidetes.** This maximum-likelihood tree was
587 inferred from a concatenated alignment of 43 proteins using the LG+G+I model of amino-acid
588 evolution. Branch supports were calculated using a Chi2-based parametric approximate
589 likelihood-ratio test. Chlorobi species were used as outgroup. Names in bold included MAGs
590 recovered in the present study.

591 **Figure S10: Phylogenomic tree of the Chloroflexi, Saccharibacteria and Microgenomates.**
592 This maximum-likelihood tree was inferred from a concatenated alignment of 43 proteins using
593 the LG+G+I+F model of amino-acid evolution. Branch supports were calculated using a Chi2-
594 based parametric approximate likelihood-ratio test. Actinobacteria species were used as
595 outgroup. Names in bold included MAGs recovered in the present study.

596 **Figure S11: Phylogenomic tree of the Synergistetes.** This maximum-likelihood tree was
597 inferred from a concatenated alignment of 43 proteins using the LG+G+I+F model of amino-acid
598 evolution. Branch supports were calculated using a Chi2-based parametric approximate
599 likelihood-ratio test. Elusimicrobia species were used as outgroup. Names in bold included
600 MAGs recovered in the present study.

601 **Figure S12: Phylogenomic tree of the Planctomycetes.** This maximum-likelihood tree was
602 inferred from a concatenated alignment of 43 proteins using the LG+G+I+F model of amino-acid
603 evolution. Branch supports were calculated using a Chi2-based parametric approximate
604 likelihood-ratio test. Verrucomicrobia species were used as outgroup. Names in bold included
605 MAGs recovered in the present study.

606 **Figure S13: Phylogenomic tree of the Elusimicrobia.** This maximum-likelihood tree was
607 inferred from a concatenated alignment of 43 proteins using the LG+G+I+F model of amino-acid
608 evolution. Branch supports were calculated using a Chi2-based parametric approximate

609 likelihood-ratio test. Spirochaetes species were used as outgroup. Names in bold included MAGs
610 recovered in the present study.

611 **Figure S14: Phylogenomic tree of the Cloacimonetes.** This maximum-likelihood tree was
612 inferred from a concatenated alignment of 43 proteins using the LG+G+I+F model of amino-acid
613 evolution. Branch supports were calculated using a Chi2-based parametric approximate
614 likelihood-ratio test. Fibrobacteres species were used as outgroup. Names in bold included
615 MAGs recovered in the present study.

616 **Figure S15: Phylogenomic tree of the Kiritimatiellaeota.** This maximum-likelihood tree was
617 inferred from a concatenated alignment of 43 proteins using the LG+G+I model of amino-acid
618 evolution. Branch supports were calculated using a Chi2-based parametric approximate
619 likelihood-ratio test. Chlamydiae species were used as outgroup. Names in bold included MAGs
620 recovered in the present study.

621 **Figure S16: Phylogenomic tree of the Acidobacteria.** This maximum-likelihood tree was
622 inferred from a concatenated alignment of 43 proteins using the LG+G+I+F model of amino-acid
623 evolution. Branch supports were calculated using a Chi2-based parametric approximate
624 likelihood-ratio test. Proteobacteria species were used as outgroup. Names in bold included
625 MAGs recovered in the present study.

626

627 References

- 628 Abdul Rahman N, Parks DH, Vanwonderghem I, Morrison M, Tyson GW, Hugenholtz P. 2016.
629 A phylogenomic analysis of the bacterial phylum Fibrobacteres. *Frontiers in Microbiology*
630 6. DOI: 10.3389/fmicb.2015.01469.
- 631 Abdul Rahman N, Parks DH, Willner DL, Engelbrektson AL, Goffredi SK, Warnecke F,
632 Scheffrahn RH, Hugenholtz P. 2015. A molecular survey of Australian and North American
633 termite genera indicates that vertical inheritance is the primary force shaping termite gut
634 microbiomes. *Microbiome* 3:5. DOI: 10.1186/s40168-015-0067-8.
- 635 Albertsen M, Hugenholtz P, Skarshewski A, Nielsen KL, Tyson GW, Nielsen PH. 2013.
636 Genome sequences of rare, uncultured bacteria obtained by differential coverage binning of
637 multiple metagenomes. *Nature Biotechnology* 31:533–538. DOI: 10.1038/nbt.2579.
- 638 Anisimova M, Gascuel O. 2006. Approximate likelihood-ratio test for branches: A fast, accurate,
639 and powerful alternative. *Systematic biology* 55:539–52. DOI:
640 10.1080/10635150600755453.
- 641 Asnicar F, Weingart G, Tickle TL, Huttenhower C, Segata N. 2015. Compact graphical
642 representation of phylogenetic data and metadata with GraPhlAn. *PeerJ* 3:e1029. DOI:

- 643 10.7717/peerj.1029.
- 644 Bourguignon T, Lo N, Dietrich C, Šobotník J, Sidek S, Roisin Y, Brune A, Evans TA. 2018.
645 Rampant host switching shaped the termite gut microbiome. *Current Biology* 28:649-
646 654.e2. DOI: 10.1016/j.cub.2018.01.035.
- 647 Bowers RM, Kyrpides NC, Stepanauskas R, Harmon-Smith M, Doud D, Reddy TBK, Schulz F,
648 Jarett J, Rivers AR, Eloë-Fadrosh EA, Tringe SG, Ivanova NN, Copeland A, Clum A,
649 Becraft ED, Malmstrom RR, Birren B, Podar M, Bork P, Weinstock GM, Garrity GM,
650 Dodsworth JA, Yooseph S, Sutton G, Glöckner FO, Gilbert JA, Nelson WC, Hallam SJ,
651 Jungbluth SP, Ettema TJG, Tighe S, Konstantinidis KT, Liu W-T, Baker BJ, Rattei T, Eisen
652 JA, Hedlund B, McMahon KD, Fierer N, Knight R, Finn R, Cochrane G, Karsch-Mizrachi
653 I, Tyson GW, Rinke C, Kyrpides NC, Schriml L, Garrity GM, Hugenholtz P, Sutton G,
654 Yilmaz P, Meyer F, Glöckner FO, Gilbert JA, Knight R, Finn R, Cochrane G, Karsch-
655 Mizrachi I, Lapidus A, Meyer F, Yilmaz P, Parks DH, Eren AM, Schriml L, Banfield JF,
656 Hugenholtz P, Woyke T. 2017. Minimum information about a single amplified genome
657 (MISAG) and a metagenome-assembled genome (MIMAG) of bacteria and archaea. *Nature*
658 *Biotechnology* 35:725–731. DOI: 10.1038/nbt.3893.
- 659 Brune A. 2014. Symbiotic digestion of lignocellulose in termite guts. *Nature Reviews*
660 *Microbiology* 12:168–180. DOI: 10.1038/nrmicro3182.
- 661 Brune A. 2018. *Methanogenesis in the digestive tracts of insects and other arthropods*. Berlin,
662 Heidelberg, Heidelberg: Springer Berlin Heidelberg. DOI: 10.1007/978-3-540-77587-4.
- 663 Brune A, Dietrich C. 2015. The gut microbiota of termites: Digesting the diversity in the light of
664 ecology and evolution. *Annual Review of Microbiology* 69:145–166. DOI:
665 10.1146/annurev-micro-092412-155715.
- 666 Bushnell B. 2014. *BBMap: a fast, accurate, splice-aware aligner*. DOI: 10.1186/1471-2105-13-
667 238.
- 668 Capella-Gutierrez S, Silla-Martinez JM, Gabaldon T, Capella-Gutiérrez S, Silla-Martínez JM,
669 Gabaldón T. 2009. trimAl: a tool for automated alignment trimming in large-scale
670 phylogenetic analyses. *Bioinformatics* 25:1972–1973. DOI: 10.1093/bioinformatics/btp348.
- 671 Ceja-Navarro JA, Nguyen NH, Karaoz U, Gross SR, Herman DJ, Andersen GL, Bruns TD, Pett-
672 Ridge J, Blackwell M, Brodie EL. 2014. Compartmentalized microbial composition,
673 oxygen gradients and nitrogen fixation in the gut of *Odontotaenius disjunctus*. *The ISME*
674 *journal* 8:6–18. DOI: 10.1038/ismej.2013.134.
- 675 Cragg SM, Beckham GT, Bruce NC, Bugg TD, Distel DL, Dupree P, Etxabe AG, Goodell BS,
676 Jellison J, McGeehan JE, McQueen-Mason SJ, Schnorr K, Walton PH, Watts JE, Zimmer
677 M. 2015. Lignocellulose degradation mechanisms across the Tree of Life. *Current Opinion*

- 678 *in Chemical Biology* 29:108–119. DOI: 10.1016/j.cbpa.2015.10.018.
- 679 Dahlsjö CAL, Parr CL, Malhi Y, Meir P, Chevarria OVC, Eggleton P. 2014. Termites promote
680 soil carbon and nitrogen depletion: Results from an *in situ* macrofauna exclusion
681 experiment, Peru. *Soil Biology and Biochemistry* 77:109–111. DOI:
682 10.1016/j.soilbio.2014.05.033.
- 683 DeAngelis KM, Allgaier M, Chavarria Y, Fortney JL, Hugenholtz P, Simmons B, Sublette K,
684 Silver WL, Hazen TC. 2011. Characterization of trapped lignin-degrading microbes in
685 tropical forest soil. *PLoS One* 6:e19306. DOI: 10.1371/journal.pone.0019306.
- 686 Delmont TO, Quince C, Shaiber A, Esen ÖC, Lee ST, Rappé MS, McLellan SL, Lückner S, Eren
687 AM. 2018. Nitrogen-fixing populations of Planctomycetes and Proteobacteria are abundant
688 in surface ocean metagenomes. *Nature Microbiology* 3:804–813. DOI: 10.1038/s41564-
689 018-0176-9.
- 690 Dietrich C, Brune A. 2016. The complete mitogenomes of six higher termite species
691 reconstructed from metagenomic datasets (*Cornitermes* sp., *Cubitermes ugandensis*,
692 *Microcerotermes parvus*, *Nasutitermes corniger*, *Neocapritermes taracua*, and *Termes*
693 *hospes*). *Mitochondrial DNA* 27:3903–3904. DOI: 10.3109/19401736.2014.987257.
- 694 Dietrich C, Kohler T, Brune A. 2014. The cockroach origin of the termite gut microbiota:
695 Patterns in bacterial community structure reflect major evolutionary events. *Applied and*
696 *Environmental Microbiology* 80:2261–2269. DOI: 10.1128/AEM.04206-13.
- 697 Diouf M, Hervé V, Mora P, Robert A, Frechault S, Rouland-Lefèvre C, Miambi E. 2018a.
698 Evidence from the gut microbiota of swarming alates of a vertical transmission of the
699 bacterial symbionts in *Nasutitermes arborum* (Termitidae, Nasutitermitinae). *Antonie van*
700 *Leeuwenhoek* 111:573–587. DOI: 10.1007/s10482-017-0978-4.
- 701 Diouf M, Miambi E, Mora P, Frechault S, Robert A, Rouland-Lefèvre C, Hervé V. 2018b.
702 Variations in the relative abundance of *Wolbachia* in the gut of *Nasutitermes arborum*
703 across life stages and castes. *FEMS Microbiology Letters* 365. DOI: 10.1093/femsle/fny046.
- 704 Donovan SE, Eggleton P, Bignell DE. 2001. Gut content analysis and a new feeding group
705 classification of termites. *Ecological Entomology* 26:356–366. DOI: 10.1046/j.1365-
706 2311.2001.00342.x.
- 707 Friedrich MW, Schmitt-Wagner D, Lueders T, Brune A. 2001. Axial differences in community
708 structure of Crenarchaeota and Euryarchaeota in the highly compartmentalized gut of the
709 soil-feeding termite *Cubitermes orthognathus*. *Applied and Environmental Microbiology*
710 67:4880–4890. DOI: 10.1128/AEM.67.10.4880-4890.2001.
- 711 Fujita A, Miura T, Matsumoto T. 2008. Differences in cellulose digestive systems among castes
712 in two termite lineages. *Physiological Entomology* 33:73–82. DOI: 10.1111/j.1365-

- 713 3032.2007.00606.x.
- 714 Graber JR, Leadbetter JR, Breznak JA. 2004. Description of *Treponema azotonutricium* sp. nov.
715 and *Treponema primitia* sp. nov., the first spirochetes isolated from termite guts. *Applied*
716 *and Environmental Microbiology* 70:1315–1320. DOI: 10.1128/AEM.70.3.1315-
717 1320.2004.
- 718 Grech-Mora I, Fardeau M-L, Patel BKC, Ollivier B, Rimbault A, Prensier G, Garcia J-L,
719 Garnier-Sillam E. 1996. Isolation and characterization of *Sporobacter termitidis* gen. nov.,
720 sp. nov., from the digestive tract of the wood-feeding termite *Nasutitermes lujae*.
721 *International Journal of Systematic Bacteriology* 46:512–518. DOI: 10.1099/00207713-46-
722 2-512.
- 723 Griffiths HM, Ashton LA, Evans TA, Parr CL, Eggleton P. 2019. Termites can decompose more
724 than half of deadwood in tropical rainforest. *Current Biology* 29:R118–R119. DOI:
725 10.1016/j.cub.2019.01.012.
- 726 Guindon S, Dufayard JF, Lefort V, Anisimova M, Hordijk W, Gascuel O. 2010. New algorithms
727 and methods to estimate maximum-likelihood phylogenies: Assessing the performance of
728 PhyML 3.0. *Systematic Biology* 59:307–321. DOI: 10.1093/sysbio/syq010.
- 729 Gupta RS, Mahmood S, Adeolu M. 2013. A phylogenomic and molecular signature based
730 approach for characterization of the phylum Spirochaetes and its major clades: proposal for
731 a taxonomic revision of the phylum. *Frontiers in microbiology* 4:217. DOI:
732 10.3389/fmicb.2013.00217.
- 733 He S, Ivanova N, Kirton E, Allgaier M, Bergin C, Scheffrahn RH, Kyripides NC, Warnecke F,
734 Tringe SG, Hugenholtz P. 2013. Comparative metagenomic and metatranscriptomic
735 analysis of hindgut paunch microbiota in wood- and dung-feeding higher termites. *PloS one*
736 8:e61126. DOI: 10.1371/journal.pone.0061126.
- 737 Herlemann DPR, Geissinger O, Ikeda-Ohtsubo W, Kunin V, Sun H, Lapidus A, Hugenholtz P,
738 Brune A. 2009. Genomic analysis of “*Elusimicrobium minutum*” the first cultivated
739 representative of the phylum “Elusimicrobia” (formerly termite group 1). *Applied and*
740 *Environmental Microbiology* 75:2841–2849. DOI: 10.1128/AEM.02698-08.
- 741 Hervé V, Brune A. 2017. The complete mitochondrial genomes of the higher termites
742 *Labiatermes labralis* and *Embiratermes neotenicus* (Termitidae: Syntermitinae).
743 *Mitochondrial DNA Part B* 2:109–110. DOI: 10.1080/23802359.2017.1289349.
- 744 Hervé V, Le Roux X, Uroz S, Gelhaye E, Frey-Klett P. 2014. Diversity and structure of bacterial
745 communities associated with *Phanerochaete chrysosporium* during wood decay.
746 *Environmental Microbiology* 16:2238–2252. DOI: 10.1111/1462-2920.12347.
- 747 Hongoh Y, Deevong P, Hattori S, Inoue T, Noda S, Noparatnaraporn N, Kudo T, Ohkuma M.

- 748 2006. Phylogenetic diversity, localization, and cell morphologies of members of the
749 candidate phylum TG3 and a subphylum in the phylum Fibrobacteres, recently discovered
750 bacterial groups dominant in termite guts. *Applied and Environmental Microbiology*
751 72:6780–8. DOI: 10.1128/AEM.00891-06.
- 752 Hongoh Y, Deevong P, Inoue T, Moriya S, Trakulnaleamsai S, Ohkuma M, Vongkaluang C,
753 Noparatnaraporn N, Kudo T. 2005. Intra- and interspecific comparisons of bacterial
754 diversity and community structure support coevolution of gut microbiota and termite host.
755 *Applied and environmental microbiology* 71:6590–9. DOI: 10.1128/AEM.71.11.6590-
756 6599.2005.
- 757 Hongoh Y, Sharma VK, Prakash T, Noda S, Taylor TD, Kudo T, Sakaki Y, Toyoda A, Hattori
758 M, Ohkuma M. 2008a. Complete genome of the uncultured Termite Group 1 bacteria in a
759 single host protist cell. *Proceedings of the National Academy of Sciences* 105:5555–5560.
760 DOI: 10.1073/pnas.0801389105.
- 761 Hongoh Y, Sharma VK, Prakash T, Noda S, Toh H, Taylor TD, Kudo T, Sakaki Y, Toyoda A,
762 Hattori M, Ohkuma M. 2008b. Genome of an endosymbiont coupling N₂ fixation to
763 cellulolysis within protist cells in termite gut. *Science (New York, N.Y.)* 322:1108–9. DOI:
764 10.1126/science.1165578.
- 765 Kang DD, Li F, Kirton E, Thomas A, Egan R, An H, Wang Z. 2019. MetaBAT 2: an adaptive
766 binning algorithm for robust and efficient genome reconstruction from metagenome
767 assemblies. *PeerJ* 7:e7359. DOI: 10.7717/peerj.7359.
- 768 Katoh K, Standley DM. 2013. MAFFT multiple sequence alignment software version 7:
769 improvements in performance and usability. *Molecular Biology and Evolution* 30:772–80.
770 DOI: 10.1093/molbev/mst010.
- 771 Köhler T, Dietrich C, Scheffrahn RH, Brune A. 2012. High-resolution analysis of gut
772 environment and bacterial microbiota reveals functional compartmentation of the gut in
773 wood-feeding higher termites (*Nasutitermes* spp.). *Applied and environmental microbiology*
774 78:4691–701. DOI: 10.1128/AEM.00683-12.
- 775 Köhler T, Stingl U, Meuser K, Brune A. 2008. Novel lineages of Planctomycetes densely
776 colonize the alkaline gut of soil-feeding termites (*Cubitermes* spp.). *Environmental*
777 *Microbiology* 10:1260–1270. DOI: 10.1111/j.1462-2920.2007.01540.x.
- 778 Krishna K, Grimaldi DA, Krishna V, Engel MS. 2013. Treatise on the Isoptera of the World.
779 *Bulletin of the American Museum of Natural History* 377:2433–2705. DOI: 10.1206/377.7.
- 780 Kuhnigk T, Branke J, Krekeler D, Cypionka H, König H. 1996. A feasible role of sulfate-
781 reducing bacteria in the termite gut. *Systematic and Applied Microbiology* 19:139–149.
782 DOI: 10.1016/S0723-2020(96)80039-7.

- 783 Lazar CS, Baker BJ, Seitz K, Hyde AS, Dick GJ, Hinrichs K-U, Teske AP. 2016. Genomic
784 evidence for distinct carbon substrate preferences and ecological niches of Bathyarchaeota
785 in estuarine sediments. *Environmental Microbiology* 18:1200–1211. DOI: 10.1111/1462-
786 2920.13142.
- 787 Leadbetter JR, Schmidt TM, Graber JR, Breznak JA. 1999. Acetogenesis from H₂ plus CO₂ by
788 spirochetes from termite guts. *Science (New York, N.Y.)* 283:686–9.
- 789 Lefort V, Longueville J-E, Gascuel O. 2017. SMS: Smart Model Selection in PhyML. *Molecular*
790 *Biology and Evolution* 6:461–464. DOI: 10.1093/molbev/msx149.
- 791 Letunic I, Bork P. 2019. Interactive Tree Of Life (iTOL) v4: recent updates and new
792 developments. *Nucleic Acids Research*. DOI: 10.1093/nar/gkz239.
- 793 Li H, Durbin R. 2009. Fast and accurate short read alignment with Burrows-Wheeler transform.
794 *Bioinformatics (Oxford, England)* 25:1754–60. DOI: 10.1093/bioinformatics/btp324.
- 795 Li H, Handsaker B, Wysoker A, Fennell T, Ruan J, Homer N, Marth G, Abecasis G, Durbin R.
796 2009. The Sequence Alignment/Map format and SAMtools. *Bioinformatics* 25:2078–2079.
797 DOI: 10.1093/bioinformatics/btp352.
- 798 Lilburn, Schmidt, Breznak. 1999. Phylogenetic diversity of termite gut spirochaetes.
799 *Environmental Microbiology* 1:331–345. DOI: 10.1046/j.1462-2920.1999.00043.x.
- 800 Liu G, Cornwell WK, Cao K, Hu Y, Van Logtestijn RSP, Yang S, Xie X, Zhang Y, Ye D, Pan
801 X, Ye X, Huang Z, Dong M, Cornelissen JHC. 2015. Termites amplify the effects of wood
802 traits on decomposition rates among multiple bamboo and dicot woody species. *Journal of*
803 *Ecology* 103:1214–1223. DOI: 10.1111/1365-2745.12427.
- 804 Lombard V, Golaconda Ramulu H, Drula E, Coutinho PM, Henrissat B. 2014. The carbohydrate-
805 active enzymes database (CAZy) in 2013. *Nucleic Acids Research* 42:D490–D495. DOI:
806 10.1093/nar/gkt1178.
- 807 Markowitz VM, Chen I-MA, Palaniappan K, Chu K, Szeto E, Pillay M, Ratner A, Huang J,
808 Woyke T, Huntemann M, Anderson I, Billis K, Varghese N, Mavromatis K, Pati A, Ivanova
809 NN, Kyrpides NC. 2014. IMG 4 version of the integrated microbial genomes comparative
810 analysis system. *Nucleic Acids Research* 42:D560–D567. DOI: 10.1093/nar/gkt963.
- 811 Marynowska M, Goux X, Sillam-Dussès D, Rouland-Lefèvre C, Roisin Y, Delfosse P,
812 Calusinska M. 2017. Optimization of a metatranscriptomic approach to study the
813 lignocellulolytic potential of the higher termite gut microbiome. *BMC Genomics* 18:681.
814 DOI: 10.1186/s12864-017-4076-9.
- 815 Mikaelyan A, Dietrich C, Köhler T, Poulsen M, Sillam-Dussès D, Brune A. 2015a. Diet is the
816 primary determinant of bacterial community structure in the guts of higher termites.

- 817 *Molecular Ecology* 24:5284–5295. DOI: 10.1111/mec.13376.
- 818 Mikaelyan A, Köhler T, Lampert N, Rohland J, Boga H, Meuser K, Brune A. 2015b. Classifying
819 the bacterial gut microbiota of termites and cockroaches: A curated phylogenetic reference
820 database (DictDb). *Systematic and Applied Microbiology* 38:472–482. DOI:
821 10.1016/j.syapm.2015.07.004.
- 822 Mikaelyan A, Meuser K, Brune A. 2017. Microenvironmental heterogeneity of gut
823 compartments drives bacterial community structure in wood- and humus-feeding higher
824 termites. *FEMS Microbiology Ecology* 93:fiw210. DOI: 10.1093/femsec/fiw210.
- 825 Mikaelyan A, Strassert JFH, Tokuda G, Brune A. 2014. The fibre-associated cellulolytic
826 bacterial community in the hindgut of wood-feeding higher termites (*Nasutitermes* spp.).
827 *Environmental Microbiology* 16:2711–2722. DOI: 10.1111/1462-2920.12425.
- 828 Moreira EA, Alvarez TM, Persinoti GF, Paixão DAA, Menezes LR, Cairo JPF, Squina FM,
829 Costa-Leonardo AM, Carrijo T, Arab A. 2018. Microbial communities of the gut and nest
830 of the humus- and litter-feeding termite *Procornitermes araujo* (Syntermitinae). *Current*
831 *Microbiology*:1–10. DOI: 10.1007/s00284-018-1567-0.
- 832 Neumann AP, McCormick CA, Suen G. 2017. Fibrobacter communities in the gastrointestinal
833 tracts of diverse hindgut-fermenting herbivores are distinct from those of the rumen.
834 *Environmental Microbiology* 19:3768–3783. DOI: 10.1111/1462-2920.13878.
- 835 Neumann AP, Suen G. 2018. The phylogenomic diversity of herbivore-associated *Fibrobacter*
836 spp. is correlated to lignocellulose-degrading potential. *mSphere* 3:e00593-18. DOI:
837 10.1128/mSphere.00593-18.
- 838 Odelson DA, Breznak JA. 1983. Volatile fatty acid production by the hindgut microbiota of
839 xylophagous termites. *Applied and Environmental Microbiology* 45:1602–13.
- 840 Ohkuma M, Iida T, Kudo T. 1999. Phylogenetic relationships of symbiotic spirochetes in the gut
841 of diverse termites. *FEMS Microbiology Letters* 181:123–129.
- 842 Ohkuma M, Noda S, Hattori S, Iida T, Yuki M, Starns D, Inoue J, Darby AC, Hongoh Y. 2015.
843 Acetogenesis from H₂ plus CO₂ and nitrogen fixation by an endosymbiotic spirochete of a
844 termite-gut cellulolytic protist. *Proceedings of the National Academy of Sciences*
845 112:10224–10230. DOI: 10.1073/pnas.1423979112.
- 846 Ohkuma M, Noda S, Kudo T. 1999. Phylogenetic diversity of nitrogen fixation genes in the
847 symbiotic microbial community in the gut of diverse termites. *Applied and environmental*
848 *microbiology* 65:4926–34.
- 849 Ottesen EA, Leadbetter JR. 2011. Formyltetrahydrofolate synthetase gene diversity in the guts of
850 higher termites with different diets and lifestyles. *Applied and Environmental Microbiology*

- 851 77:3461–3467. DOI: 10.1128/AEM.02657-10.
- 852 Parks DH, Chuvochina M, Waite DW, Rinke C, Skarshewski A, Chaumeil P-A, Hugenholtz P.
853 2018. A standardized bacterial taxonomy based on genome phylogeny substantially revises
854 the tree of life. *Nature Biotechnology*. DOI: 10.1038/nbt.4229.
- 855 Parks DH, Imelfort M, Skennerton CT, Hugenholtz P, Tyson GW. 2015. CheckM: assessing the
856 quality of microbial genomes recovered from isolates, single cells, and metagenomes.
857 *Genome research* 25:1043–55. DOI: 10.1101/gr.186072.114.
- 858 Parks DH, Rinke C, Chuvochina M, Chaumeil P-A, Woodcroft BJ, Evans PN, Hugenholtz P,
859 Tyson GW. 2017. Recovery of nearly 8,000 metagenome-assembled genomes substantially
860 expands the tree of life. *Nature Microbiology* 2:1533–1542. DOI: 10.1038/s41564-017-
861 0012-7.
- 862 Paster BJ, Dewhirst FE, Cooke SM, Fussing V, Poulsen LK, Breznak JA. 1996. Phylogeny of
863 not-yet-cultured spirochetes from termite guts. *Applied and environmental microbiology*
864 62:347–52.
- 865 Prosser JI. 2015. Dispersing misconceptions and identifying opportunities for the use of “omics”
866 in soil microbial ecology. *Nature Reviews Microbiology* 13:439–446. DOI:
867 10.1038/nrmicro3468.
- 868 Qiu YL, Kuang XZ, Shi XS, Yuan XZ, Guo RB. 2014. *Paludibacter jiangxiensis* sp. nov., a
869 strictly anaerobic, propionate-producing bacterium isolated from rice paddy field. *Archives*
870 *of Microbiology* 196:149–155. DOI: 10.1007/s00203-013-0951-1.
- 871 Quast C, Pruesse E, Yilmaz P, Gerken J, Schweer T, Yarza P, Peplies J, Glöckner FO. 2013. The
872 SILVA ribosomal RNA gene database project: improved data processing and web-based
873 tools. *Nucleic acids research* 41:D590-6. DOI: 10.1093/nar/gks1219.
- 874 R Development Core Team. 2015. R: A Language and Environment for Statistical Computing.
- 875 Le Roes-Hill M, Rohland J, Burton S. 2011. Actinobacteria isolated from termite guts as a
876 source of novel oxidative enzymes. *Antonie van Leeuwenhoek* 100:589–605. DOI:
877 10.1007/s10482-011-9614-x.
- 878 Rossmassler K, Dietrich C, Thompson C, Mikaelyan A, Nonoh JO, Scheffrahn RH, Sillam-
879 Dussès D, Brune A. 2015. Metagenomic analysis of the microbiota in the highly
880 compartmented hindguts of six wood- or soil-feeding higher termites. *Microbiome* 3:56.
881 DOI: 10.1186/s40168-015-0118-1.
- 882 Sabree ZL, Moran NA. 2014. Host-specific assemblages typify gut microbial communities of
883 related insect species. *SpringerPlus* 3:138. DOI: 10.1186/2193-1801-3-138.
- 884 Schloss PD, Girard RA, Martin T, Edwards J, Thrash JC. 2016. Status of the Archaeal and

- 885 Bacterial census: An update. *mBio* 7:e00201-16. DOI: 10.1128/mBio.00201-16.
- 886 Schloss PD, Westcott SL, Ryabin T, Hall JR, Hartmann M, Hollister EB, Lesniewski RA,
887 Oakley BB, Parks DH, Robinson CJ, Sahl JW, Stres B, Thallinger GG, Van Horn DJ,
888 Weber CF. 2009. Introducing mothur: open-source, platform-independent, community-
889 supported software for describing and comparing microbial communities. *Applied and*
890 *Environmental Microbiology* 75:7537–7541. DOI: 10.1128/AEM.01541-09.
- 891 Schmidt O, Horn MA, Kolb S, Drake HL. 2015. Temperature impacts differentially on the
892 methanogenic food web of cellulose-supplemented peatland soil. *Environmental*
893 *Microbiology* 17:720–734. DOI: 10.1111/1462-2920.12507.
- 894 Schulz F, Eloë-Fadrosh EA, Bowers RM, Jarett J, Nielsen T, Ivanova NN, Kyrpides NC, Woyke
895 T. 2017. Towards a balanced view of the bacterial tree of life. *Microbiome* 5:140. DOI:
896 10.1186/s40168-017-0360-9.
- 897 Sczyrba A, Hofmann P, Belmann P, Koslicki D, Janssen S, Dröge J, Gregor I, Majda S, Fiedler
898 J, Dahms E, Bremges A, Fritz A, Garrido-Oter R, Jørgensen TS, Shapiro N, Blood PD,
899 Gurevich A, Bai Y, Turaev D, DeMaere MZ, Chikhi R, Nagarajan N, Quince C, Meyer F,
900 Balvočiūtė M, Hansen LH, Sørensen SJ, Chia BKH, Denis B, Froula JL, Wang Z, Egan R,
901 Don Kang D, Cook JJ, Deltel C, Beckstette M, Lemaitre C, Peterlongo P, Rizk G, Lavenier
902 D, Wu Y-W, Singer SW, Jain C, Strous M, Klingenberg H, Meinicke P, Barton MD,
903 Lingner T, Lin H-H, Liao Y-C, Silva GGZ, Cuevas DA, Edwards RA, Saha S, Piro VC,
904 Renard BY, Pop M, Klenk H-P, Göker M, Kyrpides NC, Woyke T, Vorholt JA, Schulze-
905 Lefert P, Rubin EM, Darling AE, Rattei T, McHardy AC. 2017. Critical Assessment of
906 Metagenome Interpretation—a benchmark of metagenomics software. *Nature Methods*
907 14:1063–1071. DOI: 10.1038/nmeth.4458.
- 908 Shi Y, Huang Z, Han S, Fan S, Yang H. 2015. Phylogenetic diversity of Archaea in the intestinal
909 tract of termites from different lineages. *Journal of Basic Microbiology* 55:1021–1028.
910 DOI: 10.1002/jobm.201400678.
- 911 Söllinger A, Tveit AT, Poulsen M, Noel SJ, Bengtsson M, Bernhardt J, Frydendahl Hellwing
912 AL, Lund P, Riedel K, Schleper C, Højberg O, Urich T. 2018. Holistic assessment of rumen
913 microbiome dynamics through quantitative metatranscriptomics reveals multifunctional
914 redundancy during key steps of anaerobic feed degradation. *mSystems* 3:e00038-18. DOI:
915 10.1128/mSystems.00038-18.
- 916 Spring S, Bunk B, Spröer C, Schumann P, Rohde M, Tindall BJ, Klenk H-P. 2016.
917 Characterization of the first cultured representative of Verrucomicrobia subdivision 5
918 indicates the proposal of a novel phylum. *The ISME Journal* 10:2801–2816. DOI:
919 10.1038/ismej.2016.84.

- 920 Stewart RD, Auffret MD, Warr A, Wisner AH, Press MO, Langford KW, Liachko I, Snelling TJ,
921 Dewhurst RJ, Walker AW, Roehe R, Watson M. 2018. Assembly of 913 microbial genomes
922 from metagenomic sequencing of the cow rumen. *Nature Communications* 9:870. DOI:
923 10.1038/s41467-018-03317-6.
- 924 Sujada N, Sungthong R, Lumyong S. 2014. Termite nests as an abundant source of cultivable
925 Actinobacteria for biotechnological purposes. *Microbes and Environments* 29:211–219.
926 DOI: 10.1264/jsme2.ME13183.
- 927 Svartström O, Alneberg J, Terrapon N, Lombard V, de Bruijn I, Malmsten J, Dalin A-M, EL
928 Muller E, Shah P, Wilmes P, Henrissat B, Aspeborg H, Andersson AF. 2017. Ninety-nine
929 de novo assembled genomes from the moose (*Alces alces*) rumen microbiome provide new
930 insights into microbial plant biomass degradation. *The ISME Journal* 11:2538–2551. DOI:
931 10.1038/ismej.2017.108.
- 932 Tokuda G, Lo N, Watanabe H, Arakawa G, Matsumoto T, Noda H. 2004. Major alteration of the
933 expression site of endogenous cellulases in members of an apical termite lineage. *Molecular*
934 *Ecology* 13:3219–3228. DOI: 10.1111/j.1365-294X.2004.02276.x.
- 935 Tokuda G, Mikaelyan A, Fukui C, Matsuura Y, Watanabe H, Fujishima M, Brune A. 2018.
936 Fiber-associated spirochetes are major agents of hemicellulose degradation in the hindgut of
937 wood-feeding higher termites. *Proceedings of the National Academy of Sciences*
938 115:E11996–E12004. DOI: 10.1073/pnas.1810550115.
- 939 Tokuda G, Tsuboi Y, Kihara K, Saitou S, Moriya S, Lo N, Kikuchi J. 2014. Metabolomic
940 profiling of ¹³C-labelled cellulose digestion in a lower termite: insights into gut symbiont
941 function. *Proceedings. Biological sciences / The Royal Society* 281:20140990. DOI:
942 10.1098/rspb.2014.0990.
- 943 Ueki A, Akasaka H, Suzuki D, Ueki K. 2006. *Paludibacter propionicigenes* gen. nov., sp. nov., a
944 novel strictly anaerobic, Gram-negative, propionate-producing bacterium isolated from
945 plant residue in irrigated rice-field soil in Japan. *International Journal of Systematic and*
946 *Evolutionary Microbiology* 56:39–44. DOI: 10.1099/ijs.0.63896-0.
- 947 Utami YD, Kuwahara H, Igai K, Murakami T, Sugaya K, Morikawa T, Nagura Y, Yuki M,
948 Deevong P, Inoue T, Kihara K, Lo N, Yamada A, Ohkuma M, Hongoh Y. 2019. Genome
949 analyses of uncultured TG2/ZB3 bacteria in ‘*Margulisbacteria*’ specifically attached to
950 ectosymbiotic spirochetes of protists in the termite gut. *The ISME Journal* 13:455–467.
951 DOI: 10.1038/s41396-018-0297-4.
- 952 Utami YD, Kuwahara H, Murakami T, Morikawa T, Sugaya K, Kihara K, Yuki M, Lo N,
953 Deevong P, Hasin S, Boonriam W, Inoue T, Yamada A, Ohkuma M, Hongoh Y. 2018.
954 Phylogenetic diversity and single-cell genome analysis of “*Melainabacteria*”, a non-

- 955 photosynthetic cyanobacterial group, in the termite gut. *Microbes and Environments* 33:50–
956 57. DOI: 10.1264/jsme2.ME17137.
- 957 Wang Y, Su L, Huang S, Bo C, Yang S, Li Y, Wang F, Xie H, Xu J, Song A. 2016. Diversity
958 and resilience of the wood-feeding higher termite *Mironasutitermes shangchengensis* gut
959 microbiota in response to temporal and diet variations. *Ecology and Evolution* 6:8235–
960 8242. DOI: 10.1002/ece3.2497.
- 961 Wertz JT, Kim E, Breznak JA, Schmidt TM, Rodrigues JLM. 2012. Genomic and physiological
962 characterization of the Verrucomicrobia isolate *Diplosphaera colitermitum* gen. nov., sp.
963 nov., reveals microaerophily and nitrogen fixation genes. *Applied and Environmental*
964 *Microbiology* 78:1544–1555. DOI: 10.1128/AEM.06466-11.
- 965 Wickham H. 2016. *ggplot2: Elegant graphics for data analysis*. Springer-Verlag New York.
966 DOI: 10.1007/978-3-319-24277-4.
- 967 Woyke T, Doud DFR, Schulz F. 2017. The trajectory of microbial single-cell sequencing. *Nature*
968 *Methods* 14:1045–1054. DOI: 10.1038/nmeth.4469.
- 969 Yamada A, Inoue T, Wiwatwitaya D, Ohkuma M, Kudo T, Abe T, Sugimoto A. 2005. Carbon
970 mineralization by termites in tropical forests, with emphasis on fungus combs. *Ecological*
971 *Research* 20:453–460.
- 972 Yuki M, Kuwahara H, Shintani M, Izawa K, Sato T, Starns D, Hongoh Y, Ohkuma M. 2015.
973 Dominant ectosymbiotic bacteria of cellulolytic protists in the termite gut also have the
974 potential to digest lignocellulose. *Environmental Microbiology* 17:4942–4953. DOI:
975 10.1111/1462-2920.12945.
- 976 Yuki M, Sakamoto M, Nishimura Y, Ohkuma M. 2018. *Lactococcus reticulitermitis* sp. nov.,
977 isolated from the gut of the subterranean termite *Reticulitermes speratus*. *International*
978 *Journal of Systematic and Evolutionary Microbiology* 68:596–601. DOI:
979 10.1099/ijsem.0.002549.
- 980 Zheng H, Brune A. 2015. Complete genome sequence of *Endomicrobium proavitum*, a free-
981 living relative of the intracellular symbionts of termite gut flagellates (phylum
982 Elusimicrobia). *Genome Announcements* 3:e00679-15. DOI: 10.1128/genomeA.00679-15.
- 983 Zhou Z, Pan J, Wang F, Gu J-D, Li M. 2018. Bathyarchaeota: globally distributed metabolic
984 generalists in anoxic environments. *FEMS Microbiology Reviews*. DOI: 10.1093/femsre/fuy023.
985

Figure 1

Relationship between the number of MAGs recovered and the number of assembled reads in the respective metagenomes.

The linear regression line and the Pearson correlation coefficient (r) are shown for the entire dataset.

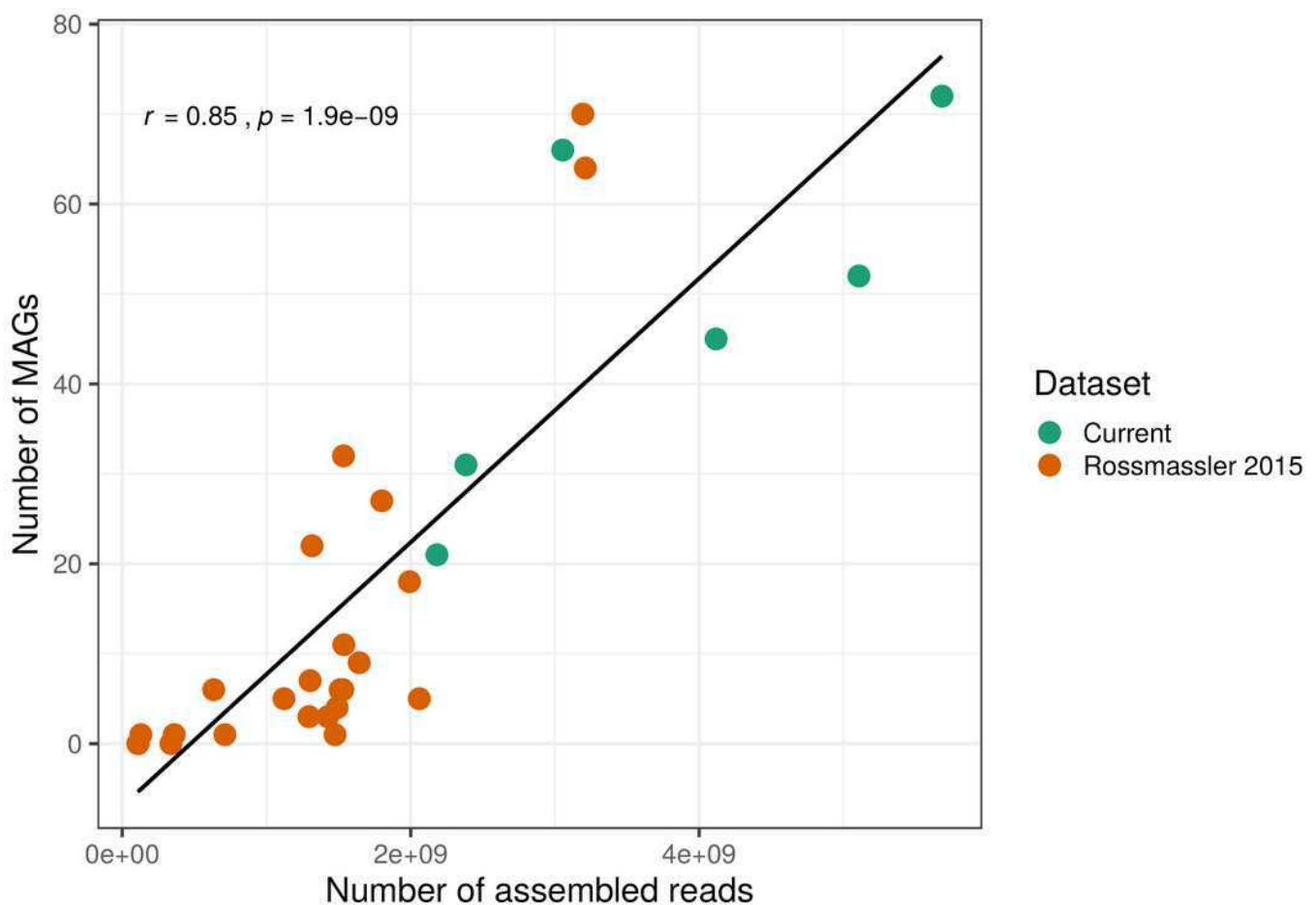


Figure 2

Distribution of the 589 MAGs among bacterial and archaeal phyla.

This maximum-likelihood tree was inferred from a concatenated alignment (amino acids) of 43 protein-coding genes using the LG+G+I model of evolution.

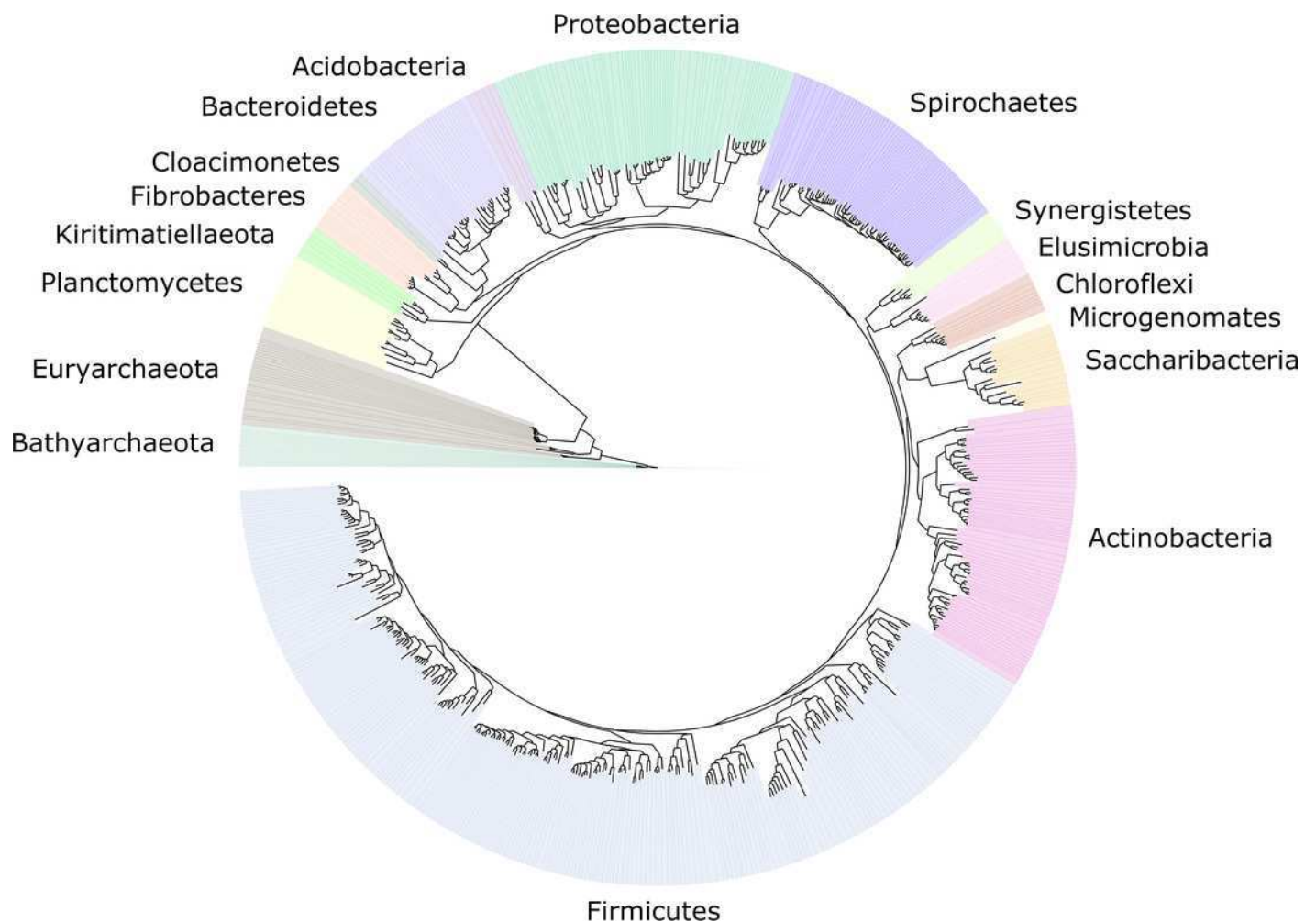


Figure 3

Relative abundance of the MAGs from different phyla among the respective metagenomes.

Circle size indicates the relative abundance of the MAGs among the respective metagenome sample; color indicates host diet.

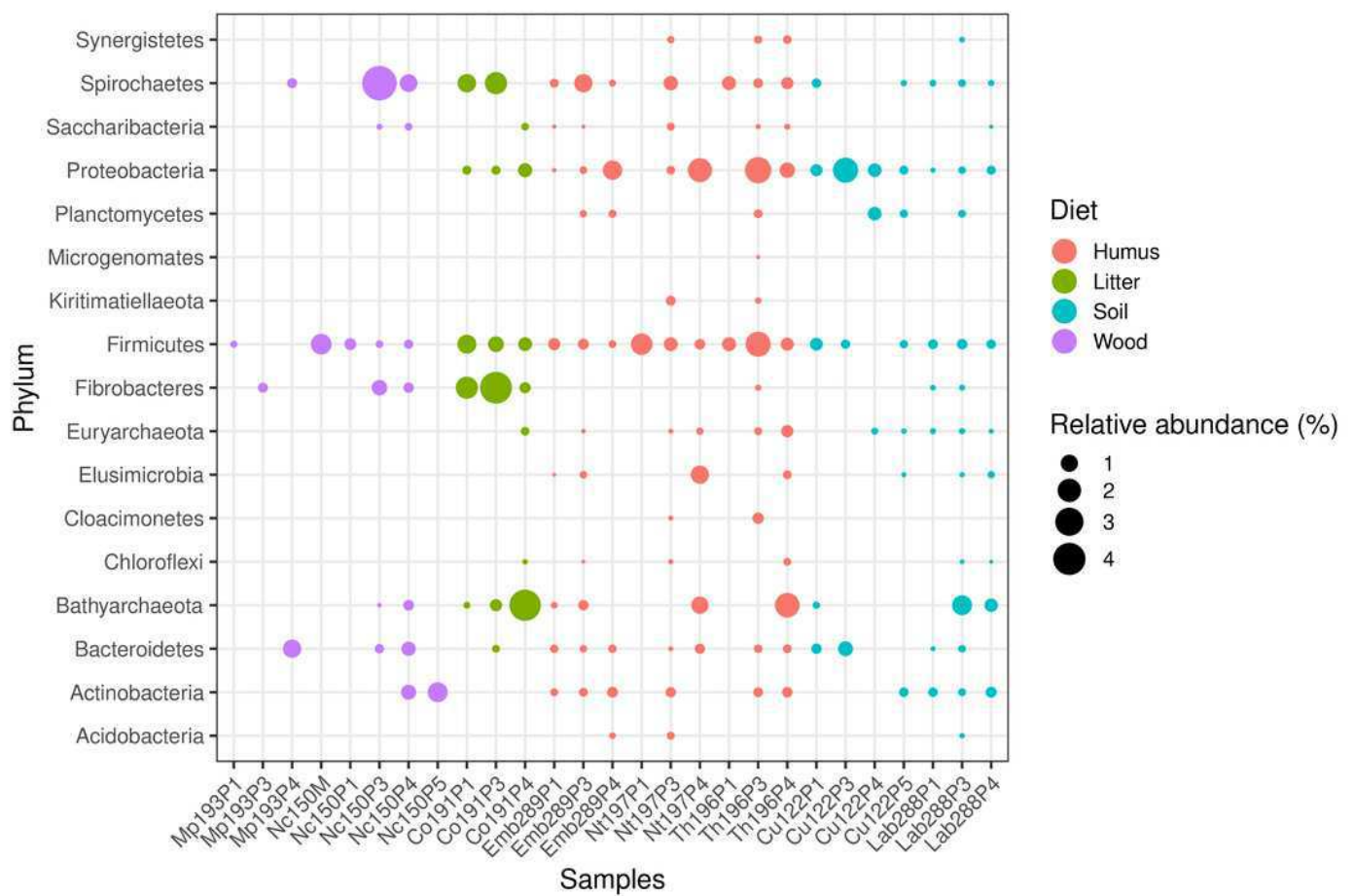


Figure 4

Phylogenomic tree of the archaeal domain.

This maximum-likelihood tree was inferred from a concatenated alignment of 43 proteins using the LG+G+I+F model of amino-acid evolution. Branch supports were calculated using a Chi2-based parametric approximate likelihood-ratio test. Names in bold included MAGs recovered in the present study. Clusters shaded in brown consist exclusively of MAGs from termite guts and clusters shaded in gray contain genomes from termite guts. The Asgard group was used as outgroup.

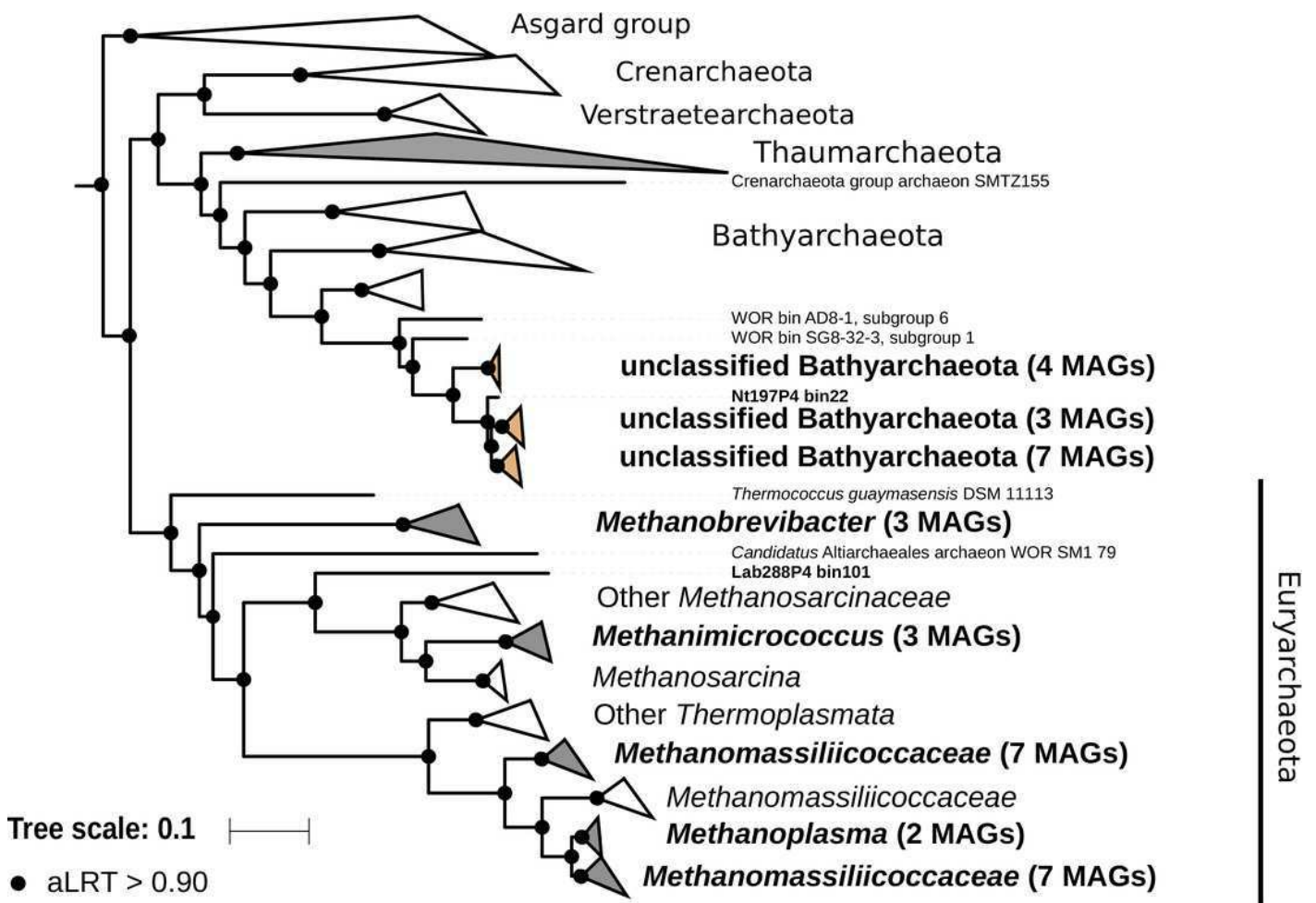


Figure 5

Phylogenomic tree of the Spirochaetes phylum.

This maximum-likelihood tree was inferred from a concatenated alignment of 43 proteins using the LG+G+I+F model of amino-acid evolution. Branch supports were calculated using a Chi2-based parametric approximate likelihood-ratio test. Names in bold included MAGs recovered in the present study. Clusters shaded in brown consist exclusively of genomes from termite guts and clusters shaded in gray contain genomes from termite guts. Elusimicrobia and Cyanobacteria were used as outgroup.

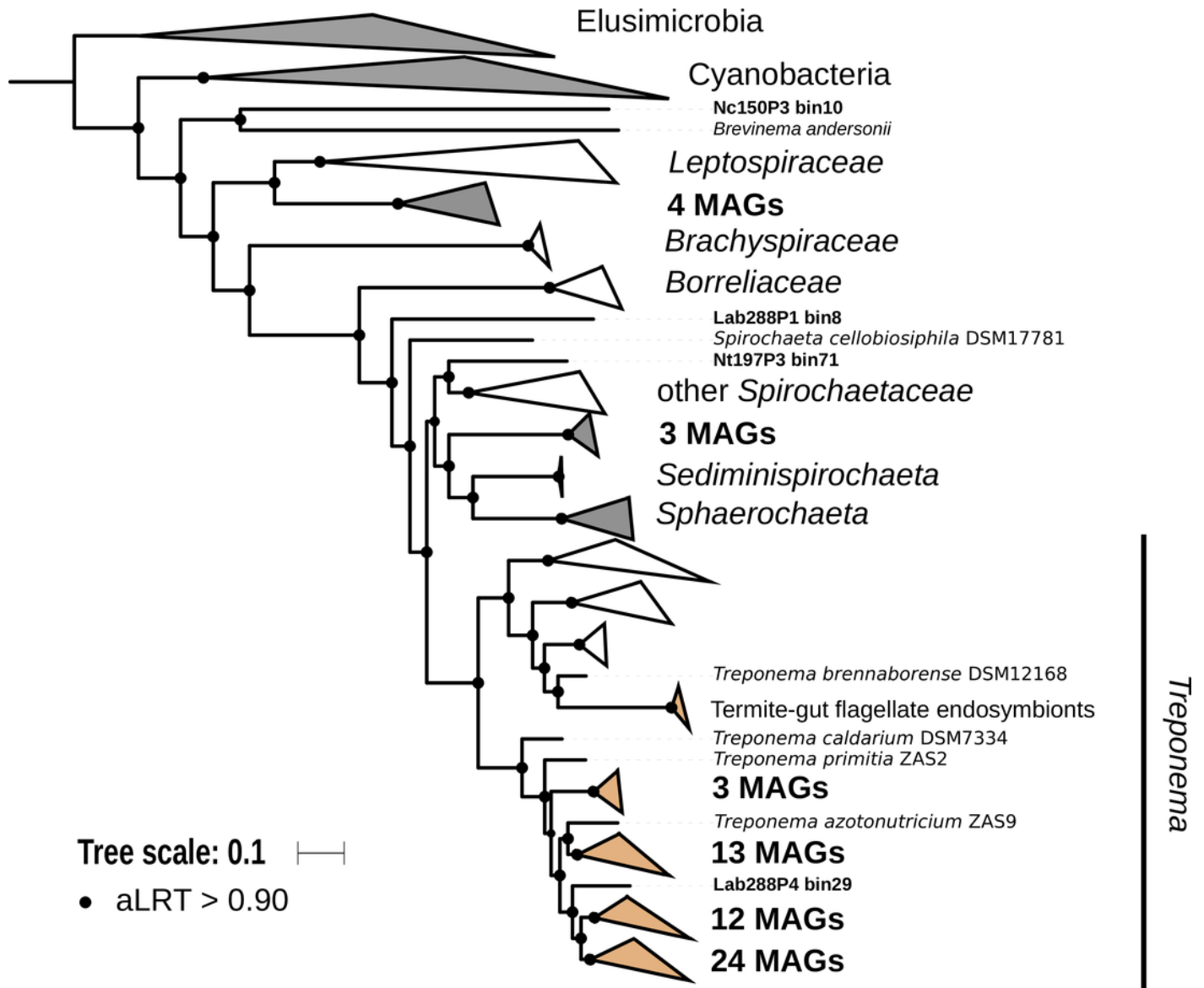


Figure 6

Phylogenomic tree of the Fibrobacteres phylum.

This maximum-likelihood tree was inferred from a concatenated alignment of 43 proteins using the LG+G+I+F model of amino-acid evolution. Branch supports were calculated using a Chi2-based parametric approximate likelihood-ratio test. Names in bold included MAGs recovered in the present study. Clusters shaded in brown consist exclusively of genomes from termite guts and clusters shaded in gray contain genomes from termite guts. Bacteroidetes were used as outgroup.

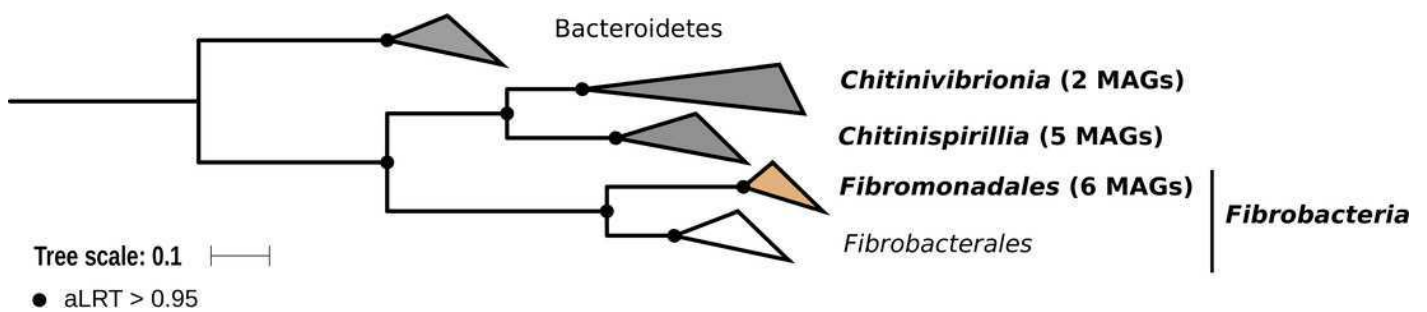


Table 1 (on next page)

Recovery of metagenome-assembled genomes (MAGs) from the 30 termite gut metagenomes analyzed in this study.

The host termite, its mitochondrial genome accession number, dietary preference, and the originating gut compartments are indicated. *C* crop (foregut), *M* midgut, *P1–P5* proctodeal compartments (hindgut). The sample codes used for the metagenomes are the combination of host ID and gut compartment.

1 **Table 1. Recovery of metagenome-assembled genomes (MAGs) from the 30 termite gut**
 2 **metagenomes analyzed in this study.** The host termite, its mitochondrial genome accession
 3 number, dietary preference, and the originating gut compartments are indicated. *C* crop (foregut),
 4 *M* midgut, *P1–P5* proctodeal compartments (hindgut). The sample codes used for the
 5 metagenomes are the combination of host ID and gut compartment.

6
7

Termite species	ID	Mitogenome	Diet	Number of MAGs						
				C	M	P1	P3	P4	P5	Total
<i>Microcerotermes parvus</i>	Mp193	KP091690	Wood	– ^a	–	1	1	4	–	6
<i>Nasutitermes corniger</i>	Nc150	KP091691	Wood	0	1	3	6	9	1	20
<i>Cornitermes</i> sp.	Co191	KP091688	Litter	–	–	32	22	7	–	61
<i>Neocapritermes taracua</i>	Nt197	KP091692	Humus	–	–	6	70	11	–	87
<i>Termes hospes</i>	Th196	KP091693	Humus	–	–	6	64	27	–	97
<i>Embiratermes neotenicus</i>	Emb289	KY436202	Humus	–	–	45	52	21	–	118
<i>Labiatermes labralis</i>	Lab288	KY436201	Soil	–	–	66	72	31	–	169
<i>Cubitermes ugandensis</i>	Cu122	KP091689	Soil	0	0	5	5	3	18	31

8
9 ^a Not sequenced.